nature reviews earth & environment

https://doi.org/10.1038/s43017-022-00379-5

Review article

Check for updates

Mineral dust aerosol impacts on global climate and climate change

Jasper F. Kok[1] ✉, Trude Storelvmo[2], Vlassis A. Karydis[3], Adeyemi A. Adebiyi[4], Natalie M. Mahowald[5], Amato T. Evan[6], Cenlin He[7] & Danny M. Leung[1]

Abstract

Mineral dust aerosols impact the energy budget of Earth through interactions with radiation, clouds, atmospheric chemistry, the cryosphere and biogeochemistry. In this Review, we summarize these interactions and assess the resulting impacts of dust, and of changes in dust, on global climate and climate change. The total effect of dust interactions on the global energy budget of Earth — the dust effective radiative effect — is -0.2 ± 0.5 W m^{-2} (90% confidence interval), suggesting that dust net cools the climate. Global dust mass loading has increased 55 ± 30% since pre-industrial times, driven largely by increases in dust from Asia and North Africa, leading to changes in the energy budget of Earth. Indeed, this increase in dust has produced a global mean effective radiative forcing of -0.07 ± 0.18 W m^{-2}, somewhat counteracting greenhouse warming. Current climate models and climate assessments do not represent the historical increase in dust and thus omit the resulting radiative forcing, biasing climate change projections and assessments of climate sensitivity. Climate model simulations of future changes in dust diverge widely and are very uncertain. Further work is thus needed to constrain the radiative effects of dust on climate and to improve the representation of dust in climate models.

Sections

[1]Department of Atmospheric and Oceanic Sciences, University of California — Los Angeles, Los Angeles, CA, USA. [2]Department of Geoscience, University of Oslo, Oslo, Norway. [3]Institute for Energy and Climate Research: Troposphere, Forschungszentrum Jülich GmbH, Jülich, Germany. [4]Department of Life and Environmental Sciences, University of California — Merced, Merced, CA, USA. [5]Department of Earth and Atmospheric Sciences, Cornell University, Ithaca, NY, USA. [6]Scripps Institution of Oceanography, University of California — San Diego, San Diego, CA, USA. [7]Research Applications Laboratory, National Center for Atmospheric Research, Boulder, CO, USA. ✉e-mail: jfkok@ucla.edu

Introduction

Mineral dust aerosols are small rock-derived particles suspended in the atmosphere with diameter, D, <~100 μm (refs. [1,2]). Most dust is produced by the ballistic impacts of wind-driven sand grains on sparsely vegetated and dry soils[3], ejecting and fragmenting soil particles[1,4]. Owing to these mechanical impacts, dust is a relatively coarse aerosol, with most of its mass contained in the coarse (D > 2.5 μm) and super-coarse (D > 10 μm) size ranges[5,6].

Dust is produced in copious amounts in the deserts of the world, with a total atmospheric loading of ~26 million tonnes, constituting a large majority of the atmospheric aerosol burden by mass[7,8]. The Sahara Desert and the Sahel contribute ~50% of global dust emissions (~2,100 Tg per year) and mass loading (~13 Tg), the Asian deserts contribute ~40% (~2,000 Tg per year and ~10 Tg) and the North American and Southern Hemisphere deserts and high-latitude regions contribute another ~10% (~500 Tg per year and ~3 Tg)[9,10] (Fig. 1). Although much of the dust is deposited close to source regions, a substantial fraction is transported vast distances. For example, plumes of African dust regularly travel across the tropical North Atlantic, reaching the southwestern USA and the Amazon Basin[11].

The abundance and long-range transport of dust cause it to impact climate through various mechanisms. During transport, dust scatters and absorbs solar shortwave (SW) and terrestrial longwave (LW) radiation[7,12], modifies cloud properties through seeding cloud droplets and ice crystals[13,14], mixes with other aerosols[15] and serves as a sink for radiatively important atmospheric trace gases[15–18]. On deposition, dust darkens snow and ice packs[19,20] and stimulates ecosystem productivity and CO_2 drawdown through the delivery of iron and phosphorus[21]. These mechanisms both cool and warm the climate system[7,15,22], the net effect of which is uncertain. Accordingly, the sign and magnitude of radiative perturbations arising from increases in dust since the pre-industrial era[23,24] are also uncertain, meaning that it is unknown whether dust changes have enhanced or opposed anthropogenic warming.

In this Review, we examine the impacts of dust, and of changes in dust, on global climate and climate change. We first summarize the various mechanisms through which dust impacts the radiation budget of Earth and assess the radiative effect produced by each mechanism. We then constrain the increase in dust loading since pre-industrial times and assess the radiative perturbation produced by this historical increase in dust. We further discuss the radiative perturbation arising from possible future changes in dust, before ending with recommendations for future research priorities.

Mechanisms by which dust impacts climate

Dust perturbs the energy balance of the Earth through various mechanisms. In each case, a radiative effect is produced, defined as the imbalance between incoming net solar radiation and outgoing infrared radiation at the top of atmosphere (TOA), resulting from the presence of an atmospheric constituent (in this case, dust)[25]. These effects can be either instantaneous, such as scattering and absorbing SW and LW radiation, or an adjustment, such as altering cloud cover[26].

We calculate the radiative effect in the modernclimate from mechanism i, r_i (W m^{-2}), as the change in the energy balance of the Earth, Δf_i (W m^{-2}), produced per change in global dust mass loading from

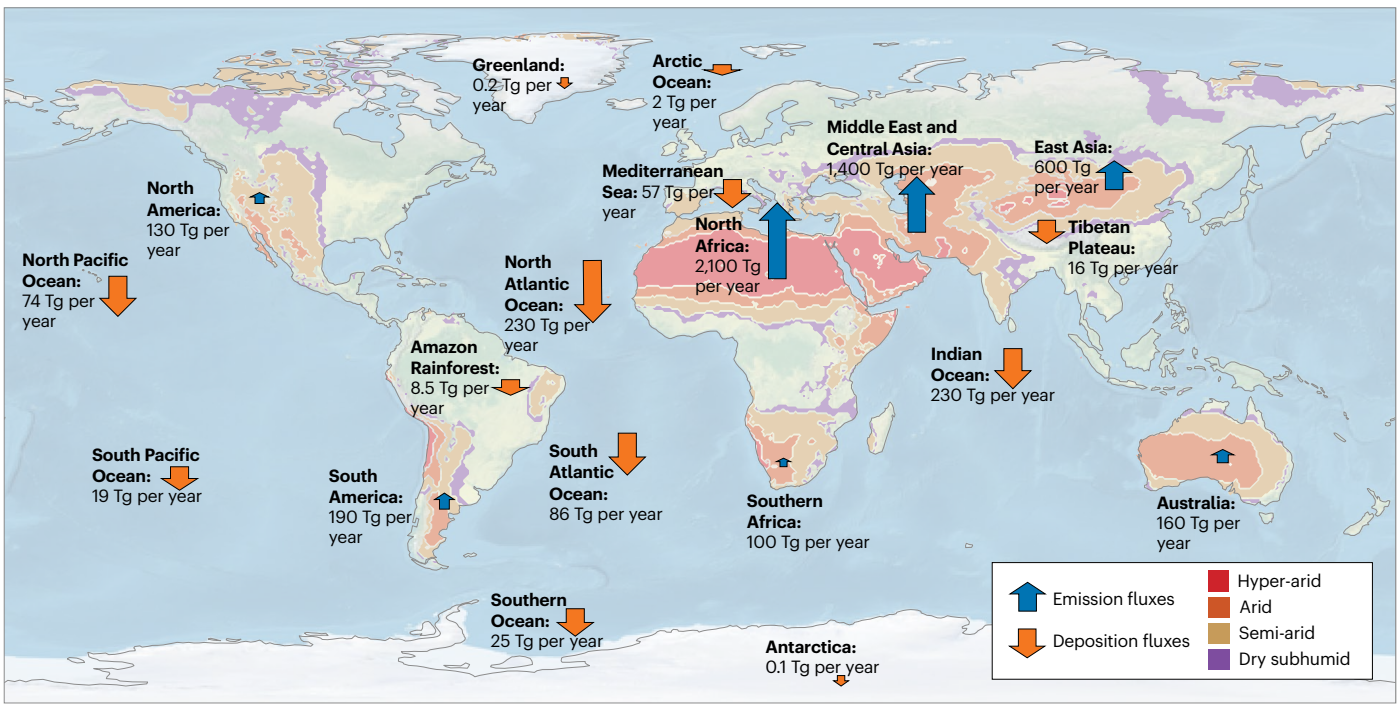

Fig. 1 | Sources and sinks of dust in the global dust cycle. Emission fluxes (blue arrows) from the main dust source regions of the world, and deposition fluxes (orange arrows) in regions where dust impacts surface albedo or biogeochemistry. Fluxes are for dust with geometric (volume-equivalent) diameter up to 20 μm and are based on constraints for 2004–2008 (ref. [42]); emissions from high-latitude regions are not included. Shading represents dryland classification on the basis of the aridity index (AI): hyper-arid regions (AI < 0.05; red shading), arid regions (0.05 < AI < 0.20; orange shading), semi-arid regions (0.20 < AI < 0.50; light-brown shading) and dry subhumid regions (0.50 < AI < 0.65; purple shading)[203]. Most dust is emitted from drylands in North Africa and Asia, collectively known as the 'dust belt'.

modern levels, ΔL_i (Tg), multiplied by the global modern dust loading, L (Tg). That is,

$$r_i \equiv \frac{\Delta f_i}{\Delta L_i} L \quad (1)$$

The sum of all radiative effects then equals the effective radiative effect of dust, R (W m^{-2}), which includes instantaneous radiative effects and adjustments[26,27]:

$$R = \sum_i r_i \quad (2)$$

Equations (1) and (2) define the dust effective radiative effect such that it can be used to obtain the radiative perturbation, ΔF, owing to a change in dust loading, ΔL_m, from its value in the modern climate:

$$\Delta F = R \frac{\Delta L_m}{L} \quad (3)$$

The effective radiative forcing of dust arising from the change in dust mass loading over pre-industrial to modern times, $\Delta L_{p \to m}$, can then be defined as

$$\Delta F_{p \to m} = R \frac{\Delta L_{p \to m}}{L} \quad (4)$$

Use of the term radiative forcing here deviates slightly from previous work[26,27], in which it denotes radiative perturbations entirely from anthropogenic forcing agents. However, because dust is a natural aerosol affected by climate changes and human land-use changes, a radiative perturbation from historical changes in dust can be partially related to human land-use changes (a forcing) and natural and anthropogenic climate changes (a feedback). These two contributions are difficult to disentangle, and so the entire radiative perturbation arising from historical changes in dust is referred to as the dust effective radiative forcing.

Radiative effects from dust arise through interactions with radiation, atmospheric chemistry, clouds, the cryosphere and biogeochemistry (Fig. 2). Each of these mechanisms are now discussed.

Interactions with radiation

The best understood mechanism by which dust impacts climate is through the dust direct radiative effect (DRE), the perturbation of the energy balance of Earth by scattering and absorption of radiation (Fig. 2a). As dust sizes vary from ~0.1 to 100 μm[28], it interacts with SW (centred around 550 nm wavelength) and LW (centred around 10 μm wavelength) radiation[29,30].

The sign and magnitude of the dust DRE depend on the balance between these interactions. For instance, scattering of SW radiation cools the climate, whereas SW absorption warms the climate; the overall net effect is cooling[7,31]. By contrast, scattering and absorption of LW radiation warms the climate as both decrease the transparency of the atmosphere to terrestrial LW radiation[32]. Thus, the balance between cooling from SW scattering and warming from SW absorption and LW scattering and absorption dictate the dust DRE.

For SW radiation, the balance between scattering and absorption is influenced by dust particle size. Absorption increases more strongly with particle size than scattering, and so the single-scattering albedo (SSA, the ratio of scattered radiation to total extinguished radiation) decreases with particle size. Indeed, submicron dust has an SSA close to 1, whereas supermicron dust absorbs a substantial fraction of the extinguished radiation, exhibiting SSAs of ~0.95 at D = 2 μm, ~0.80 at D = 10 μm and even lower for super-coarse dust[29,33].

However, the exact SSA of dust aerosols depends on their complex refractive index, determined by particle mineralogy[30]. Absorption increases approximately linearly with iron oxide content, primarily provided by hematite and goethite[34]. Dust optical properties can also be affected by mixing with other aerosols, especially black carbon[35]. Observations suggest that this mixing has a limited impact on the optical properties of most African dust[36,37], but could substantially affect those of East Asian dust[38].

Although dust particle size and mineralogy determine the balance between SW scattering and absorption, the efficiency with which these processes perturb the TOA radiative flux depends on the albedo of the underlying surface. Indeed, the cooling effect of SW scattering is enhanced if the dust is situated above dark (low albedo) surfaces, such as the ocean and forests, that would otherwise absorb most of the radiation[39]. Conversely, the warming effect of SW absorption is enhanced if the dust is situated above clouds or above high albedo land surfaces, such as snow, ice and deserts, that would otherwise scatter most of the radiation back to space[40,41].

Dust microphysical properties and mineralogy also influence the extinction of LW radiation. For example, with its longer wavelengths, LW radiation is extinguished primarily by coarse dust[29,32,42]. The sensitivity of LW extinction to mineralogy is less important than for SW interactions owing to the smaller variability in LW optical properties between minerals and because LW scattering and absorption both warm the planet[30,43,44].

The efficiency with which dust extinction of LW radiation perturbs the TOA radiative flux also depends on the transparency of the atmosphere to LW radiation and the elevation of the dust layer. Indeed, the TOA flux is only substantially impacted if the atmosphere is at least somewhat transparent to LW radiation, as is the case in the absence of clouds in the ~8–13 μm 'atmospheric window'[32,45]. Furthermore, because LW emission depends on temperature, LW warming depends on the temperature difference between the dust layer and the source of the LW radiation — usually the surface or clouds below the dust layer. In addition, the transparency of the atmosphere to LW radiation decreases with the concentration of water vapour and thus increases with height. As such, dust warming by LW extinction increases approximately linearly with the height of the dust layer[32,39,45,46].

Although the processes by which dust interacts with SW and LW radiation are relatively well understood, the resulting radiative effects are poorly constrained. For dust interactions with SW radiation, central estimates of SW DRE are −0.40 W m^{-2} (−0.10 to −0.70 W m^{-2}, 90% confidence interval)[7,31,47–51] (Fig. 3); these estimates are based on assessments that used optical properties and dust size distributions that are consistent with experimental constraints[4,6,7,28,34,37,52,53]. The wide range reflects substantial uncertainties in the dust size distribution[7] and optical properties[44].

Best estimates of LW DRE are +0.25 W m^{-2} with a range of +0.10 to +0.40 W m^{-2} (refs. [7,31,44,47–50]) (Fig. 3); these estimates use realistic optical properties[43] and size distributions that are consistent with satellite constraints on the LW DRE[46,54]. The range reflects uncertainties in dust LW optical properties[43], the height of dust plumes[55,56], the dust size distribution and contribution of super-coarse dust[33,47,52] and the effect of LW scattering by dust (the latter is neglected in climate models[31,32] and is sometimes accounted for using a simple correction factor[7,31,44,50]).

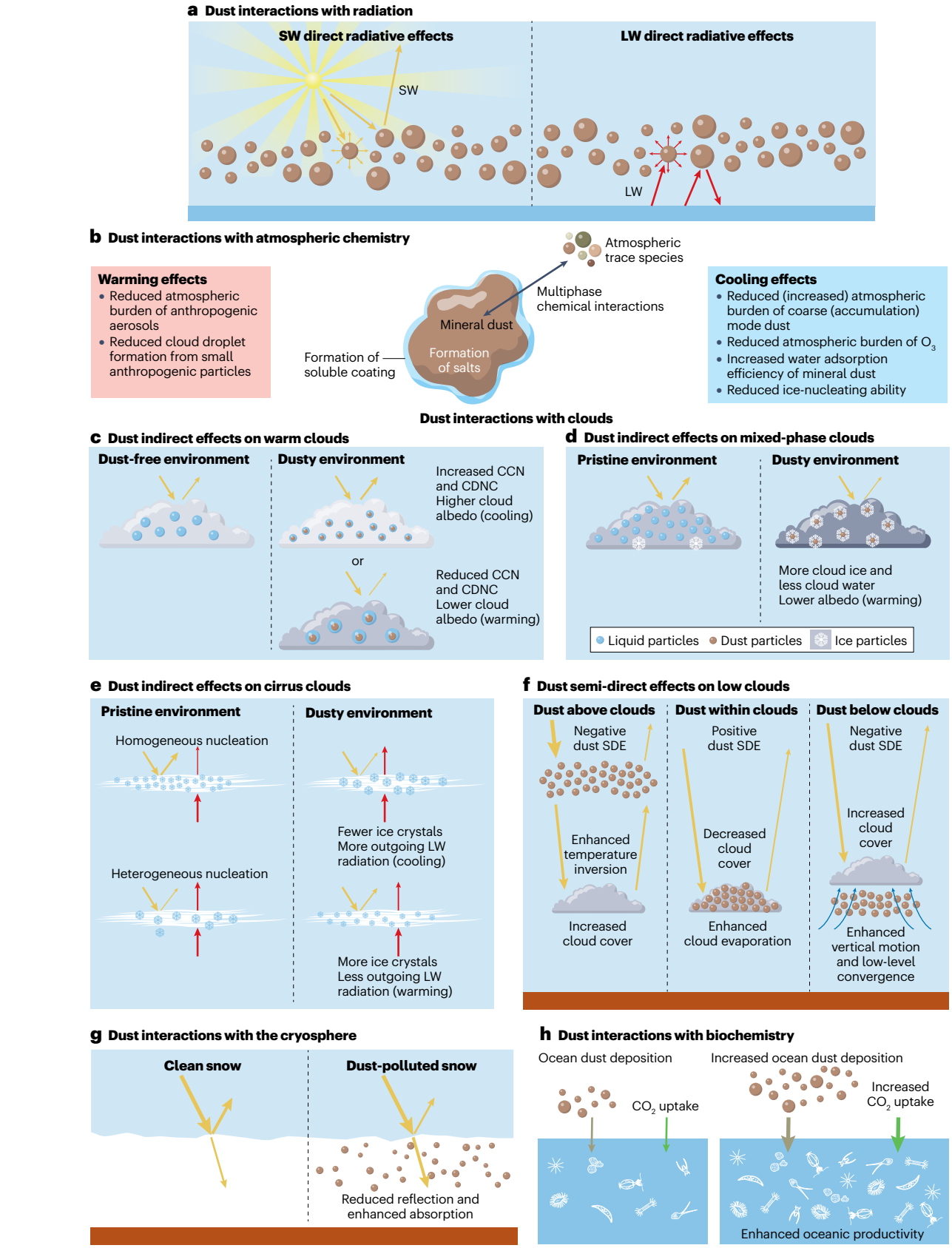
a Dust interactions with radiation
SW direct radiative effects
LW direct radiative effects
SW
LW
b Dust interactions with atmospheric chemistry
Warming effects
• Reduced atmospheric burden of anthropogenic aerosols
• Reduced cloud droplet formation from small anthropogenic particles
Atmospheric trace species
Multiphase chemical interactions
Mineral dust
Formation of soluble coating
Formation of salts
Cooling effects
• Reduced (increased) atmospheric burden of coarse (accumulation) mode dust
• Reduced atmospheric burden of O_3
• Increased water adsorption efficiency of mineral dust
• Reduced ice-nucleating ability
Dust interactions with clouds
c Dust indirect effects on warm clouds
Dust-free environment
Dusty environment
Increased CCN and CDNC Higher cloud albedo (cooling)
or
Reduced CCN and CDNC Lower cloud albedo (warming)
d Dust indirect effects on mixed-phase clouds
Pristine environment
Dusty environment
More cloud ice and less cloud water Lower albedo (warming)
Liquid particles
Dust particles
Ice particles
e Dust indirect effects on cirrus clouds
Pristine environment
Dusty environment
Homogeneous nucleation
Heterogeneous nucleation
Fewer ice crystals More outgoing LW radiation (cooling)
More ice crystals Less outgoing LW radiation (warming)
f Dust semi-direct effects on low clouds
Dust above clouds
Dust within clouds
Dust below clouds
Negative dust SDE
Positive dust SDE
Negative dust SDE
Enhanced temperature inversion
Decreased cloud cover
Increased cloud cover
Increased cloud cover
Enhanced cloud evaporation
Enhanced vertical motion and low-level convergence
g Dust interactions with the cryosphere
Clean snow
Dust-polluted snow
Reduced reflection and enhanced absorption
h Dust interactions with biochemistry
Ocean dust deposition
Increased ocean dust deposition
CO_2 uptake
Increased CO_2 uptake
Enhanced oceanic productivity

Fig. 2 | Mechanisms through which dust impacts climate. a, Dust direct interactions with shortwave (SW; yellow) and longwave (LW; red) radiation. **b**, Dust interactions with atmospheric chemistry and their corresponding warming or cooling effects. **c**, Dust indirect effects on warm clouds via modifications to cloud condensation nuclei (CCN) and cloud droplet number concentration (CDNC). **d**, Dust indirect effects on mixed-phase clouds via changes in the partitioning of cloud water between liquid and solid phases. **e**, Dust indirect effects on cirrus clouds, separated by the dominant ice crystal formation mechanism in the absence of dust, occurring through dust changing the number and size of ice crystals. **f**, Dust semi-direct effect (SDE) on low clouds, separated by location of dust relative to clouds, owing to local heating generated by dust absorption. **g**, Radiative effects of dust deposited on snow and ice through changes in reflectivity and absorption. **h**, Effect of dust on CO_2 drawdown via interactions with ocean biogeochemistry. Dust affects climate through a wide range of mechanisms that alternately cool and warm the climate, making the magnitude and sign of the net radiative effect of dust on climate uncertain. Parts **d** and **e** adapted with permission from ref. [13], Annual Reviews.

It is thus unclear whether the dust DRE exerts a net cooling or warming effect. Combining the SW and LW DRE yields a net dust DRE of -0.15 ± 0.35 W m^{-2}, consistent with other calculations[7,31,44,47–49] (Fig. 3). As such, the dust DRE could either slightly warm or substantially cool the planet, or it could have little net impact. We assign medium confidence to this assessment owing to the large body of research and availability of satellite-based constraints.

Interactions with atmospheric chemistry

Dust affects atmospheric chemistry through interactions with atmospheric trace gases and aerosols. Although freshly emitted mineral dust is considered insoluble, it is reactive towards trace acidic gases derived from anthropogenic pollutants and sea salt. Mineral dust particles are notably associated with nitrate[57,58]. Nitric acid interacts with the non-volatile mineral cations of dust, forming salts to maintain the charge balance in the aerosol phase[59]. The uptake of such acidic vapours is rapid owing to simple acid–base interactions with carbonates and other minerals[60]. Over continents, such interactions of mineral cations with anthropogenic sulfuric acid cause the accumulation of substantial amounts of sulfate on dust surfaces[61]. By contrast, over oceans, mineral cations are commonly associated with chloride derived from sea salt[62].

Mineral dust also provides surfaces for the adsorption of inorganic (notably SO_2, NO_2 and O_3) and organic trace gases[18], influencing the optical properties, hygroscopicity and atmospheric residence time of dust and anthropogenic aerosols. Therefore, dust particles provide a substantial sink for the direct removal of important atmospheric constituents such as O_3, affecting the oxidative capacity of the atmosphere and ozone radiative forcing[63,64]. Dust particles also provide reaction sites for the oxidation of SO_2 to sulfuric acid[65] and for the formation of nitrous acid through heterogeneous reactions of NO_2 (ref. [66]). However, given that acid anhydrides do not initially contain any acidic protons[60], such heterogeneous formation of salts occurs at a much slower pace than through the direct uptake of acidic vapours. Additionally, high pH values on alkaline mineral particles can promote the formation of ammonium nitrate on their surface[67,68]. These dust–gas interactions transform the surface and even the bulk chemical composition of dust particles[69,70]. This chemical processing is highly dependent on the gas phase composition and the dust chemical composition[59,71], the latter influenced by source soil mineralogy[72].

The chemical ageing of dust through these reactions creates a soluble coating that increases hydrophilicity, which in turn affects dust residence time and interactions with clouds. For example, the interaction of a calcite-containing dust particle with nitric acid converts the insoluble calcium carbonate to the highly hygroscopic calcium nitrate[73]. The enhanced hygroscopicity increases water adsorption efficiency, accelerating growth under humid conditions, thus causing more efficient cloud droplet formation and extinction of radiation. On the contrary, increased water uptake by the large, aged dust particles depletes in-cloud supersaturation, thereby reducing the number of smaller anthropogenic particles that are activated and grow into cloud droplets[14]. Chemical ageing of mineral dust can further reduce its ice-nucleating ability[74].

These heterogeneous and multiphase reactions affect the atmospheric loading of both dust and non-dust aerosols. Nitrate formation associated with the mineral cations removes nitric acid from the gas phase, decreasing the formation of ammonium nitrate aerosols[59]. Similarly, sulfate formation on dust decreases SO_2 abundance and thus the formation of sulfate aerosols[17]. As such, dust can reduce the concentration of anthropogenic cloud condensation nuclei (CCN) by adsorption of precursor gases and coagulation with anthropogenic aerosols. The hygroscopic growth of aged dust can also increase its scavenging and deposition rate, reducing its atmospheric residence time and loading[16,75]. However, modelling suggests that these effects enhance the total accumulation mode dust burden through a reduced loss by coagulation with coarse dust particles[16].

The physicochemical interactions of mineral dust with atmospheric composition thus influence the direct and indirect radiative forcing of dust and non-dust aerosols (Fig. 2b). These effects can be negative or positive depending on the region and the prevailing impacts on aerosol loading and composition[16,17]. For example, the enhanced burden of the accumulation mode dust aerosols and the decreased absorption of SW radiation owing to the modified aerosol composition have been linked to a net cooling effect of -0.05 W m^{-2} (ref. [16]). However, observations of dust during transport indicate that the size distribution of dust with diameters <5 μm remains remarkably constant and that the optical properties change little[6,36,37]. Moreover, a critical effect of heterogeneous chemistry on dust surfaces is to reduce the atmospheric loading of anthropogenic aerosols, thereby decreasing their direct radiative cooling, resulting in a net warming of +0.12 to +0.20 W m^{-2} (refs. [17,76,77]).

Overall, the impact of dust interactions with atmospheric chemistry on the aerosol DRE is highly uncertain. The resulting radiative effect is assessed at 0.10 ± 0.15 W m^{-2} (Fig. 3), encompassing the possibility of slight cooling[16] as a lower bound and larger warming[17,76,77] as an upper bound. We assign very low confidence to this assessment.

Interactions with clouds

Dust particles influence clouds by changing the thermodynamic environment and by serving as CCN and ice-nucleating particles (INPs). Radiative perturbations produced by dust effects on warm clouds, mixed-phase clouds, cirrus (ice) clouds and by semi-direct effects (SDEs) are now discussed.

Dust indirect effects on warm clouds. There are three main pathways through which dust particles affect warm clouds: increasing the concentration of CCN, with unprocessed mineral dust possessing a modest

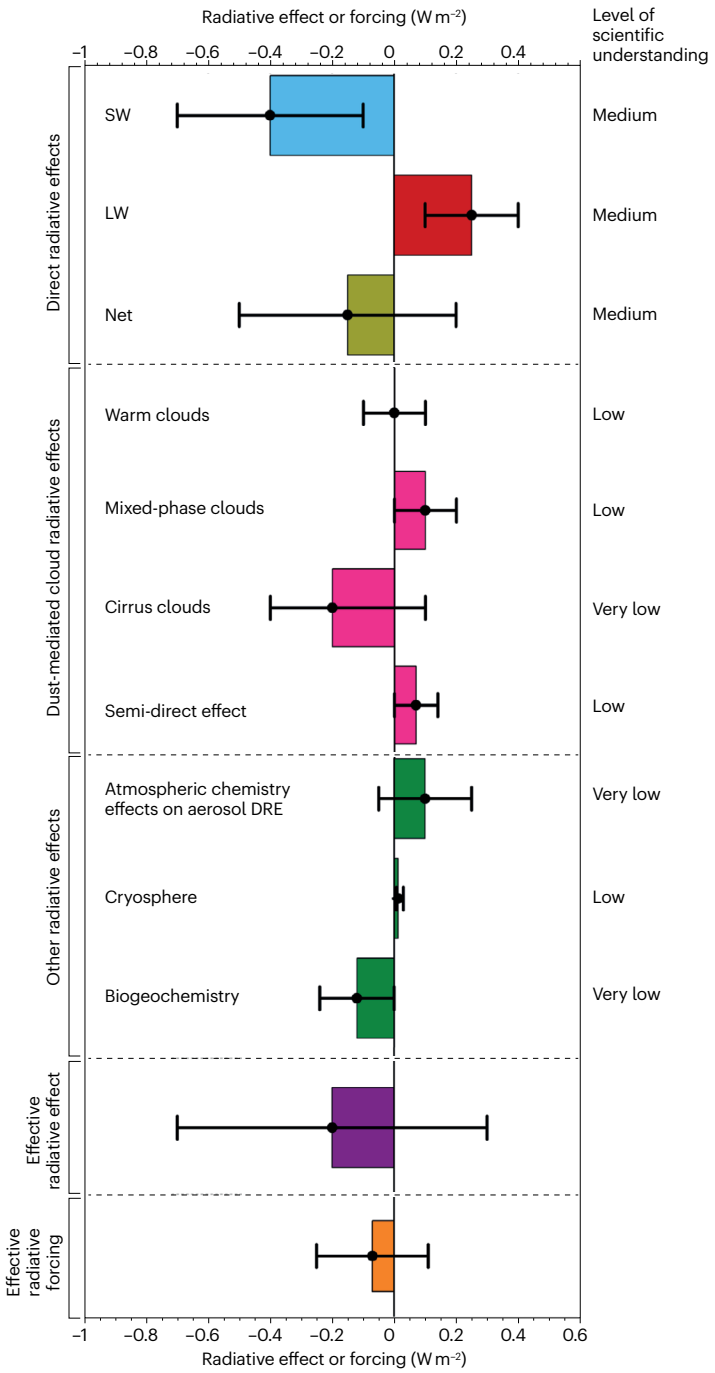

Fig. 3 | Global mean radiative effects and forcing of dust at the top of atmosphere. Dust-related perturbations to the radiation budget through direct radiative effects, dust-mediated cloud radiative effects (pink bars), other radiative effects (green bars), their sum (effective radiative effect; purple bar) and the proportion of the latter linked to dust increases since pre-industrial times (effective radiative forcing; orange bar). Error bars denote the 90% confidence range. The level of scientific understanding describes confidence in the assessment of each radiative effect, following past practice[27]. The global mean dust effective radiative effect and radiative forcing are uncertain in sign and magnitude, but are more likely to cool the climate than to warm the climate. SW, shortwave; LW, longwave.

ability to act as CCN[78,79], further enhanced by ageing[80]; reducing the concentration of non-dust CCN through coagulation and adsorption of precursor gases; and acting as giant CCN, forming cloud droplets at relatively low supersaturation and thus depleting water vapour such that overall cloud droplet formation is suppressed.

These different pathways have opposing effects: the first increases cloud droplet number concentrations (CDNCs), enhancing cloud albedo and lifetime and producing a net cooling effect. By contrast, the second and third pathways reduce CDNC, and thereby cloud albedo and lifetime, producing a net warming effect (Fig. 2c). Some modelling suggests that the pathways that lower CDNC dominate, decreasing the global mean CDNC by as much as 11% (ref. [14]). However, most modelling indicates that dust slightly increases global mean CDNC abundance, albeit with large differences in magnitude[22,81,82]. For example, global simulations with CAM5 (ref. [22]) suggest that a threefold increase in dust emissions increases CDNC by ~1%, which in turn produces a negative

forcing of −0.01 W m^{-2}. Such an effect is supported by estimates based on satellite observations[83].

Although the net global effects of dust on warm clouds are contradictory, there is broad agreement that the sign and magnitude of the dust contribution to CDNC are highly heterogeneous in space and time[14,22]. Given this disagreement and the relatively sparse research, the corresponding perturbation to TOA radiation budget of Earth through changes to liquid clouds is likely to be negative but close to zero, with an uncertainty range of −0.10 to +0.10 W m^{-2} (Fig. 3). This assessment is based on scaling the estimates of CDNC changes[14,22,81,82] with the forcing estimate per change in CDNC[22]. We assign low confidence to this assessment.

Dust indirect effects on mixed-phase clouds. Although the ability of dust to act as CCN is somewhat ambiguous, their ice-nucleating ability is undisputed[84,85]. Dust particles are efficient INPs, including in the immersion mode (freezing cloud droplets from within) relevant to mixed-phase clouds. Mixed-phase clouds have temperatures between approximately −38 and 0 °C, consisting of supercooled liquid droplets, ice crystals or a mixture of both. As such, they are generally optically thick and efficiently reflect incoming SW radiation with a cooling effect. However, their optical thickness also allows absorption of virtually all outgoing LW radiations, reducing the amount of LW radiation emitted to space and so causing a warming effect. The SW effect dominates in the global mean[86].

In an INP-limited (pristine) environment, mixed-phase clouds will be optically thick and usually have liquid cloud tops[87], with only small amounts of ice residing in the cloud interior or below cloud base (Fig. 2d). By contrast, in a dust-enriched environment, mixed-phase clouds will be partly or completely glaciated depending on the dust abundance and INP efficiency. This cloud glaciation results in an overall reduction of cloud albedo and thus a positive (warming) radiative effect (Fig. 2d).

An increase in dust loading therefore probably produces a warming effect by reducing the cooling effect of mixed-phase clouds. Modelling of these effects generally agree qualitatively but differ quantitatively. For example, global simulations with E3SM[88] found TOA radiation budget perturbations owing to the total atmospheric dust loading of +0.05 to +0.26 W m^{-2}. For comparison, CAM5 estimates that going from a very pristine state with only 10% of current dust emissions to present-day dust emissions induces a perturbation of only 0.01–0.10 W m^{-2} through dust-INP effects on mixed-phase clouds[22]; as the atmospheric dust loading change is smaller than in E3SM, these estimates are broadly consistent. These modelling results are further supported by satellite observations, indicating that dust-enriched environments tend to have mixed-phase clouds with a larger proportion of ice than their dust-free counterparts[89,90]. Thus, a perturbation to the TOA radiation budget of approximately 0.10 W m^{-2} from dust effects on mixed-phase clouds is supported, but with a relatively large assessed uncertainty range of 0–0.20 W m^{-2} (Fig. 3). We assign low confidence in this assessment owing to limited research.

Dust indirect effects on cirrus clouds. Dust particles are also the dominant INP for the formation of cirrus cloud[91,92] — pure ice clouds residing in the upper troposphere at temperatures below approximately −38 °C. In these clouds, dust particles act as INPs in the deposition mode, in which ice nucleation occurs through vapour deposition, possibly triggered by freezing of condensed water in dust particle pores[93]. Cirrus clouds reduce emission of LW radiation to space more effectively than they reflect SW radiation and thus have a net warming effect[94]. Cirrus clouds form through homogeneous or heterogeneous nucleation[85]. For homogeneous nucleation, small solution droplets freeze spontaneously, requiring high supersaturation but no INPs, typically resulting in high concentrations of small ice crystals[13]. For heterogeneous nucleation, crystals form on INPs, requiring modest supersaturation but sufficient INPs, typically resulting in low concentrations of large ice crystals. The transition from homogeneous to heterogeneous freezing is estimated to occur at INP concentrations between 10 and 100 L^{-1} (ref. [95]).

The impact of dust on cirrus clouds is highly dependent on whether non-dust INPs are present. In conditions that favour homogeneous freezing (low INP concentration), additional dust shifts nucleation to occurring heterogeneously, reducing the number of ice crystals and increasing their size[13] (Fig. 2e). This scenario would make cirrus clouds optically thinner and reduce their lifetime. By contrast, in conditions that favour heterogeneous freezing (high INP concentration), additional dust INPs would add ice crystals and reduce their size, making cirrus clouds optically thicker and extend their lifetimes[13] (Fig. 2e). Perturbations to the TOA radiation budget would be opposite in these two scenarios, and at present it is unclear which effect dominates globally.

However, model simulations incorporating up-to-date laboratory results of ice nucleation on dust particles[93,96] generally find that adding dust results in optical thinning of cirrus clouds. This thinning yields large opposing perturbations to both LW and SW radiations at the TOA, but the LW effect tends to dominate, producing net cooling[22,97]. Using CAM5, the corresponding overall radiative effect is estimated at −0.4 W m^{-2} (ref. [97]). However, simulations with a more moderate dust change (going from 10% to 100% of the present emissions) with a modified version of the same model[22] suggest a range from −0.32 to +0.05 W m^{-2}. Thus, the perturbation of the TOA radiation budget owing to dust effects on cirrus clouds is assessed at −0.20 W m^{-2}, with a 90% confidence interval of −0.40 to +0.10 W m^{-2} (Fig. 3). We assign low confidence to this assessment because of inadequate research.

Dust semi-direct effects on clouds. Absorption of radiation by mineral dust also modifies the atmospheric temperature profile[98], changing atmospheric stability, moisture profiles and secondary circulations, in turn altering cloud distributions[99,100]. Given that dust accounts for about a third of SW absorption by all aerosols, its contribution to these processes, known as aerosol SDEs[101], is crucial to quantifying the overall dust effective radiative forcing[102,103]. The magnitude of the dust SDE, and whether it results in a positive or a negative radiative effect, is dependent on two factors: the relative position of the dust and cloud layers within the atmospheric column and the amount of radiation absorbed by the dust layer[99,100]. When dust is located above boundary-layer clouds, local heating stabilizes the boundary layer by strengthening its capping inversion, increasing build-up of moisture in the boundary layer. This increased moisture enhances cloud cover, resulting in a negative SDE[100,104] (Fig. 2f). Conversely, when dust is located within or near boundary-layer clouds, local heating results in a reduction of relative humidity, evaporating the cloud and resulting in a positive SDE[100,105] (Fig. 2f). Finally, when dust is located below boundary-layer clouds, local heating enhances convergence and available moisture, increasing cloud cover and producing a negative SDE[106,107] (Fig. 2f).

Radiation absorption by dust also generates SDEs for mid-altitude and high-altitude clouds. These SDEs involve compensation between the warming effect by dust absorption (which tends to decrease cloud cover) and an increase in moisture convergence (which tends

to increase cloud cover)[99]. Although enhanced moisture convergence can overwhelm the warming effect, resulting in increased globally averaged high-altitude cloud cover during the summer, the overall annual-mean dust SDE is to decrease high cloud cover[99,108].

Understanding of dust SDEs assumes that dust, such as other absorbing aerosols, warms the atmospheric layer in which they are present[109]. This assumption is based on evidence that dust radiative warming from SW absorption dominates over cooling from LW emission[110,111]. However, the amount of coarse dust, which emits LW radiation more strongly than fine dust, has likely been underestimated[47,53]. Because accounting for the observed abundance of coarse dust could add substantial LW radiative cooling of the atmosphere[5,31,33], the understanding of the different pathways through which dust can semi-directly impact clouds remains incomplete.

Owing to uncertainties in the pathways by which dust absorption semi-directly influences cloud cover, a global observational estimate of dust SDE is not currently available. Instead, observationally based assessments have focused on dust-dominated regions[100,105,112], revealing negative (-1.2 ± 1.4 W m^{-2}) annual dust SDE over the North Atlantic Ocean[100]. Scaling such observationally based regional dust SDE estimates to global values is difficult, given strong spatial variability and contrasting mechanisms for ocean and land[99]. In addition, accurate retrievals of dust microphysical properties are lacking from global-scale satellite and ground-based platforms[103], making it difficult to obtain global estimates of dust SDE.

In the absence of global observational estimates, climate models have reported a net positive global annual-mean dust SDE[113] varying between 0.01 and 0.16 W m^{-2} depending on the model used[22,113,114]. These positive SDE estimates are consistent with an overall decrease in cloud cover in these simulations. Although model estimates of dust SDE and cloud changes are thus relatively consistent, they could be biased by unaccounted for uncertainties in dust absorption properties, the vertical distributions of dust and clouds, an underestimate of LW radiative cooling by coarse dust and the parameterization of cloud processes[53,55,102]. Therefore, on the basis of the above model simulations, the dust SDE is estimated at 0.07 ± 0.07 W m^{-2} (Fig. 3), but with low confidence.

Interactions with the cryosphere

Dust interactions with the cryosphere impact climate via dust DRE and indirect radiative effect and by darkening snow and ice surfaces after deposition (Fig. 2g). This dust-induced snow albedo effect accelerates snow and glacier melting[19,115], triggering a strong, positive surface albedo feedback[116]. The dust-induced snow albedo effect is influenced by dust concentration in snow[117,118], dust optical properties (as determined by its size distribution and chemical composition)[118,119], dust–snow mixing state[120,121], snow grain size and shape[120], snowpack properties[122,123] and illumination conditions[118,124].

Observations indicate strong heterogeneity in dust concentrations in snow and ice and thereby large variations in associated surface radiative effects. For instance, the springtime dust-induced snow albedo effect is <0.5 W m^{-2} for the Arctic[125,126], up to 5 W m^{-2} for remote mid-latitude snowpacks (such as the Tibetan Plateau)[125,127] and about 10–50 W m^{-2} over polluted mid-latitude snowpacks (such as the US Rocky Mountains)[19,115]. In some extremely polluted mid-latitude mountains, the local instantaneous snow albedo effect can be as high as 100–300 W m^{-2} (refs. [128,129]). Owing to the stronger light penetration and hence larger light absorption by dust in aged snow, the dust-induced snow albedo effect is typically larger in aged snow than in fresh snow[19].

There are only limited estimates of the global annual-mean dust-induced snow albedo effect, with a central forcing of +0.013 W m^{-2} and a 90% confidence interval of 0.007–0.03 W m^{-2} (refs. [20,117,130]) (Fig. 3). These estimates are associated with large uncertainties owing to complicated and poorly constrained dust–snowpack–radiation interactions. Indeed, variations in dust–snow mixing state, snow grain shape, dust size distribution and dust chemical composition can cause up to a factor of 2 uncertainty in the dust-induced snow albedo effect[120,121]. Limited knowledge of dust evolution within the snowpack also adds to the uncertainty. Considering these uncertainties and limited global-scale research, we assign low confidence to the dust-induced snow albedo effect.

Interactions with biogeochemistry

Dust further influences ocean and land biogeochemistry, directly through the addition of nutrients and pollutants to ecosystems and indirectly through modifying precipitation, temperature and radiation[21]. For instance, atmospheric deposition of dust onto oceans provides iron, a limiting nutrient in high-nutrient low-chlorophyll regions[131,132] and for nitrogen-fixing organisms[133,134]. The deposition of important soluble iron has increased since pre-industrial times because of enhanced iron solubilization during transport[23,135], as well as historical increases in dust. The resulting alleviation of iron limitation increases ecosystem productivity, in turn lowering atmospheric CO_2 concentrations and its radiative forcing (Fig. 2h).

These atmospheric inputs of iron to the ocean modulate ecosystem productivity and carbon sequestration on the timescale of decades[132,136]. Ocean biogeochemical models[137,138] suggest that the increased deposition of soluble iron over the twentieth century resulted in the uptake of ~4 ppm of CO_2, producing a radiative perturbation of -0.07 ± 0.07 W m^{-2} (refs. [21,139]). As approximately half of this increase in soluble iron was estimated to be due to a simulated ~40% increase in dust over the twentieth century, the dust-biogeochemistry radiative effect is estimated at -0.12 ± 0.12 W m^{-2} (Eq. 1 and Fig. 3); this effect increases over time, and so the radiative perturbation is dependent on timescale. As this estimate is based on one study, confidence in the assessment is very low.

Dust also contains phosphorus, a limiting nutrient in some tropical forests, grasslands[140,141] and ocean ecosystems[132,142]. Indeed, phosphorus from North African dust might help maintain productivity of the Amazon rainforest[143]. However, because inputs are thought to be important on millennial timescales[144], any contribution to dust radiative forcing since pre-industrial times is likely negligible. Dust further serves as a ballast, enhancing downward transfer of organic material within the ocean; no quantitative estimates of these impacts in terms of productivity or carbon uptake feedback are currently available[145,146]. In addition, desert dust could include elements that can be toxic to ocean or land ecosystems, such as Cu, but current estimates suggest that this effect is not important to the radiation budget of Earth[147].

The dust effective radiative effect

To determine the climatic impact of past and future changes in atmospheric dust, it is critical to assess the dust effective radiative effect, R (Eq. 2) – the sum of the various dust-related radiative effects (Fig. 3). Many of these radiative effects oppose one another, resulting in a median estimate of -0.2 W m^{-2} and a 90% confidence interval of -0.7 to $+0.3$ W m^{-2}; note that some rapid adjustments were neglected in this calculation, including responses by water vapour and the lapse rate to dust DREs, but these adjustments are likely small[148]. As such,

the net effect of dust on the global radiation budget of Earth could be negligible, a substantial net cooling or a small net warming.

On regional scales and for different seasons, the dust effective radiative effect can differ substantially from its global and annual mean. This variability occurs because radiative effects are sensitive to the spatiotemporal variability in dust concentration, microphysical properties (mineralogy and size distribution) and environmental conditions (surface albedo and cloud cover). For instance, dust over reflective deserts probably produces substantial warming given the high dust concentration and coarse size distribution[5] and because reflective surfaces reduce cooling produced by SW scattering and enhance warming produced by SW absorption[40,149]. Similarly, dust likely produces net warming over snow-covered and ice-covered regions, given that the high surface albedo enhances warming produced by dust absorption of SW radiation and because dust deposition decreases the surface albedo[39,117]. By contrast, dust over oceans usually produces cooling owing to the finer dust and low ocean albedo in the visible spectrum[41]. To determine the climate impacts of dust, it is thus critical to constrain not only the global annual mean dust effective radiative effect but also its spatiotemporal pattern.

Dust radiative forcing

Given that dust has a potentially large effective radiative effect, changes in dust loading since pre-industrial times could have produced a substantial effective radiative forcing. Indeed, many deposition records reveal such increases in dust deposition, sometimes up to a quadrupling[24,150–152]. These changes can be linked to climate change and human land-use changes (Box 1).

Dust reconstruction

Combining 19 dust deposition records[24,150–152] with constraints on the modern-day dust cycle[9,42], we reconstruct the evolution of global dust mass loading since pre-industrial times (Supplementary information). This dust reconstruction uses bootstrap resampling to propagate uncertainties in the experimental deposition records and the constraints on source region-resolved deposition fluxes to each deposition site; nonetheless, errors should be interpreted as a lower bound.

This reconstruction reveals that atmospheric loading of dust with a volume-equivalent diameter <20 μm increased from 19 ± 6 Tg in the pre-industrial period (1841–1860) to 29 ± 8 Tg in the modern climate (1981–2000), representing a 55 ± 30% change (Fig. 4a). Although substantial, this increase is less than the doubling of dust suggested previously[23,24]. Asian dust is a large contributor to this global change, increasing by 74 ± 37% from 8 ± 3 to 13 ± 5 Tg (Fig. 4b).

North African dust changes are smaller, rising 46% (2–102%), from 10 ± 4 to 14 ± 4 Tg (Fig. 4c). Dust also increased 28% (−14 to 88%) in the Southern Hemisphere, from 1.2 (0.6–2.2) to 1.6 (0.9–2.5) Tg (Fig. 4d). For both African and Asian reconstructions, mass loading peaked in the 1980s and decreased thereafter, consistent with long-term dust concentration measurements, visibility records and satellite observations[153–159]. Satellite observations further suggest that global dust mass loading has been relatively stable since 2000, the end point of the reconstruction, with notable regional trends such as in Central and East Asia[160].

This large historical increase in dust mass loading is inadequately accounted for in current climate models and climate assessments. Indeed, 12 CMIP6 models with prognostic dust cycles reveal little change (2 ± 11%) in dust mass loading since pre-industrial times (Fig. 5). If the dust increase was largely driven by natural and anthropogenic climate changes, this model failure could be linked to inaccurate representation of these changes or insufficient sensitivity to changes in climate. The latter possibility is suggested by the common use of

Box 1

Drivers of the historical dust loading increase

The large historical increase in dust (Fig. 4) can be linked to natural and anthropogenic climate changes or human land-use changes[205].

Observations indicate that dust is highly sensitive to climate. Indeed, dust increased two to four times between interglacial and glacial periods[206,207] and has varied a similar amount in some regions owing to twentieth-century climate variability[153,155,158]. As such, changes in aridity, vegetation cover and wind speed arising from natural climate variability could have driven the long-term increase in dust loading, at least in part, as suggested for North Africa[153,155,208]. Anthropogenic changes to climate and atmospheric composition could have additionally affected dust loading through changes to aridity and plant fertilization at desert margins[209].

Human land-use changes, primarily the increase in the fraction of ice-free land area used for agriculture from ~9% in 1850 to ~35% in 2000 (ref. [210]), could also have increased dust emissions. This large-scale conversion of wildlands to agricultural land included many semi-arid and arid regions, where land-use changes can result in huge increases in dust emission[211–213]. Additional anthropogenic contributions to dust emissions could be related to changes in water management and the resulting drying of inland bodies of water, as with Owen's Lake in California in the early twentieth century[214] and the Aral Sea in Central Asia[215,216].

Modelling has been unable to determine whether this historical increase in dust is primarily driven by climate or land-use changes. Indeed, the fraction of the global dust burden in the current climate emitted from anthropogenically disturbed sources ranges from 0% to 50% (refs. [172,180,205,217–219]). Similarly, modelling of the effects of changes in climate and CO_2 concentrations on dust loading vary from a decrease of 20% to an increase of 60% (refs. [172,205,220]).

Although large uncertainties remain in how climate and land-use changes have contributed to the historical increase in dust loading, observational findings suggest that anthropogenic land-use change was a key driver. First, the timing of increases in dust deposition in various sedimentary records coincides with the rise of industrialized agriculture in source regions[24]. Second, satellite observations suggest that ~25% of modern dust emissions originate from regions heavily impacted by human land use[221]. This finding implies that human land-use changes have increased dust mass loading by ~33% since pre-industrial times, accounting for the majority of the 55±30% increase. Moreover, satellite observations indicate that the fraction of dust emitted from anthropogenically disturbed surfaces is substantially higher for Asian than for North African source regions[221], qualitatively consistent with historical increases. Nonetheless, additional work is needed to determine the exact causes of the historical increase in dust for each of the main dust source regions of the world.

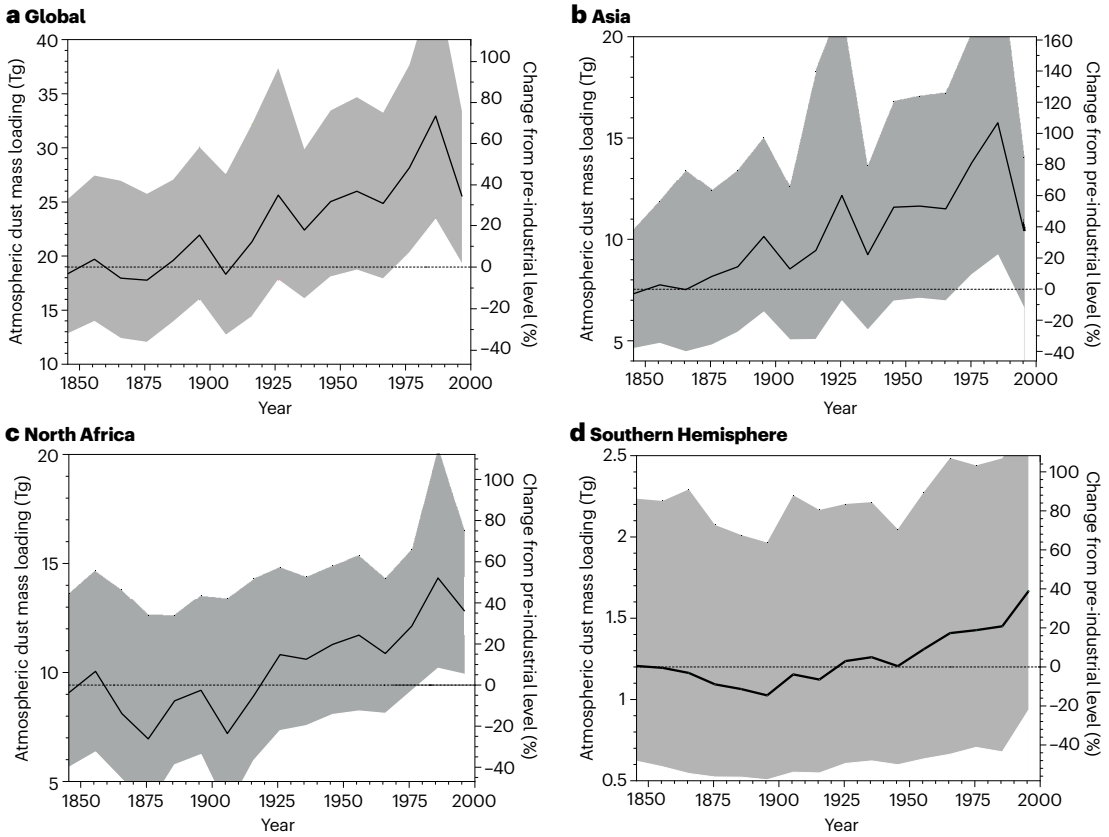

Fig. 4 | Atmospheric dust mass loading changes since pre-industrial times. **a**, Globally integrated dust mass loading reconstruction, produced by combining 19 records of dust deposition with constraints on spatially resolved dust deposition fluxes from the main dust source regions[9,42] (Supplementary information). The solid line denotes the median dust loading, shading the 90% confidence range, and the dotted line denotes the average pre-industrial (1841–1860) dust loading. **b**, As in part **a**, but for loading contributed by dust from Asia. **c**, As in part **a**, but for loading contributed by dust from North Africa. **d**, As in part **a**, but for loading contributed by dust from the Southern Hemisphere. Dust has increased in North Africa, Asia and the Southern Hemisphere, translating to a 55 ± 30% rise in global dust mass loading in modern times (1981–2000) compared with pre-industrial times.

empirical dust source functions to parameterize the spatial distribution of dust emissions[161,162], masking physical links between changeable surface properties and dust emissions[163]. Conversely, if the dust increase was driven by human land-use changes, then the model failure could be caused by an underestimation of land-use and land-cover changes in drylands and the resulting increases in dust emissions (Box 1).

Radiative forcing owing to dust increase

This historical increase in dust loading, as indicated with the reconstruction, could have produced a substantial radiative forcing. Indeed, combining an R of −0.2 ± 0.5 W m^{-2} with the 55 ± 30% historical dust loading increase yields a dust effective radiative forcing, $\Delta F_{p\rightarrow m}$, of −0.07 ± 0.18 W m^{-2} from 1841 to 2000. Dust radiative forcing could thus have substantially contributed to, or slightly opposed, the total aerosol effective radiative forcing of −1.1 (−1.7 to −0.4) W m^{-2} for 1750–2019 (ref. [164]).

These calculations of R and $\Delta F_{p\rightarrow m}$ are subject to important limitations. First, they assume that radiative effects increase linearly with aerosol loading[7,165] (Eqs. 3 and 4). However, the increase of radiative effects with aerosol loading is usually less than linear, especially for interactions with clouds and biogeochemistry[21,22,166]. Moreover, the radiative effects of dust vary in space, such that $\Delta F_{p\rightarrow m}$ depends on the spatial pattern of dust increases, which this simple calculation does not account for. For instance, Asian dust probably has an outsized impact on Northern Hemisphere cirrus clouds[91]. Moreover, high-latitude dust emissions are probably important in controlling the glaciation of mixed-phase clouds[167,168] but are not explicitly included in the dust reconstruction. Careful simulations with coupled climate models that reproduce the historical dust increase are therefore needed to better constrain dust radiative forcing.

As current climate models do not reproduce the historical dust increase, these models omit the potentially important radiative forcing from increased dust interactions with radiation, clouds, atmospheric chemistry and the cryosphere; changes in CO_2 and other greenhouse gases from dust interactions with biogeochemistry are inherently included in climate model runs forced by observed greenhouse gas concentrations. Dust radiative forcing was thus not accounted for in constraints on the total aerosol effective radiative forcing in the IPCC Sixth Assessment Report[164]. As a result, the failure by models and climate assessments to account for the historical increase in dust could have biased constraints on climate sensitivity and projections of future climate changes[169].

Future changes in dust radiative forcing

Future changes in dust radiative forcing are likely to be dominated by changes in atmospheric dust loading, which in turn will be determined by several factors. One such factor is changes in soil moisture, which are largely driven by precipitation[170] – drier soils are more susceptible to aeolian erosion owing to reduced soil cohesive forces and vegetation cover[1,2]. Increased evaporative demand over land[171] will also act to reduce soil moisture. However, the effects of reduced soil moisture could be countered by CO_2 fertilization, reducing plant water losses and thereby dust emissions by expanding vegetation into arid regions[172], although the magnitude of this effect is uncertain[173]. Terrestrial stilling, the observed downward trend in surface wind speeds over land surfaces[174], could also affect dust emissions, with models suggesting a future reduction in Northern Hemisphere winds[175]. However, changes in atmospheric circulation patterns thought to impact surface wind speeds over dust-producing regions might be more important[155]. An increase in precipitation variability[176], and thus extreme rainfall events[177], could potentially enhance sediment supply – and aeolian erosion – via alluvial and fluvial recharge[178]. Finally, future climate and land-use changes could drive a decline in biological soil crusts that reduce dust emissions, a mechanism unaccounted for in current models[179].

Model estimates of future changes in dust are sensitive to methodology[180] and range from an increase owing to increasing aridity[181] to a decrease from CO_2 fertilization[172,182]. Regional[162,183–185] and global[186] analyses of CMIP5 models reveal that the simulated dust mean state has substantial biases, that historical dust variability is not reproduced and that modelled dust emissions are insufficiently sensitive to changes in surface conditions. These simulations show no secular trends in dust over land under the high emissions RCP 8.5 scenario[186]. Many of these model deficiencies also exist in CMIP6 models (Fig. 5). Moreover, intermodel differences in dust increased relative to earlier CMIP efforts, suggesting enhanced model divergence in future projections of dust with increased model complexity[187].

Given the inability of models to reproduce historical dust changes and the large spread in projections of future dust change, estimates of changes in dust radiative forcing per degree planetary warming, the dust–climate feedback, are also uncertain. Indeed, six CMIP6 models differ in the sign of the dust–climate feedback[188], with a multimodel mean of 0.0026 ± 0.0048 W m^{-2} K^{-1}. These results are consistent with those from CMIP5, whereby the feedback was not statistically different from zero[189]. However, a feedback with the range -0.04 to $+0.02$ W m^{-2} K^{-1} is estimated when using a dust emission scheme that responds more realistically to changes in climate[190]. On a regional scale, the dust climate feedback close to source regions is likely an additional order of magnitude larger[189].

Given the lack of confidence in model projections of future changes in the dust burden, and the substantial uncertainties in dust DRE and indirect radiative effect, there is a low degree of confidence in the ability of models to predict future changes in the dust radiative forcing.

Summary and future perspectives

In the modern climate, the global mean effective radiative effect of dust, R, is estimated as -0.2 ± 0.5 W m^{-2} (Fig. 3). As such, despite considerable uncertainty in the sign and magnitude of R, which arises from the numerous uncertain and sometimes opposing mechanisms, it is more likely that dust cools the climate than warms the climate. Global dust loading also increased 55 ± 30% from pre-industrial times (Fig. 4), exerting a global mean effective radiative forcing, $\Delta F_{p \to m}$, of -0.07 ± 0.18 W m^{-2}. The historical increase in dust has therefore probably somewhat counteracted greenhouse warming. Current climate models fail to capture this historical increase in dust loading (Fig. 5) and thus inadequately account for dust radiative forcing, biasing

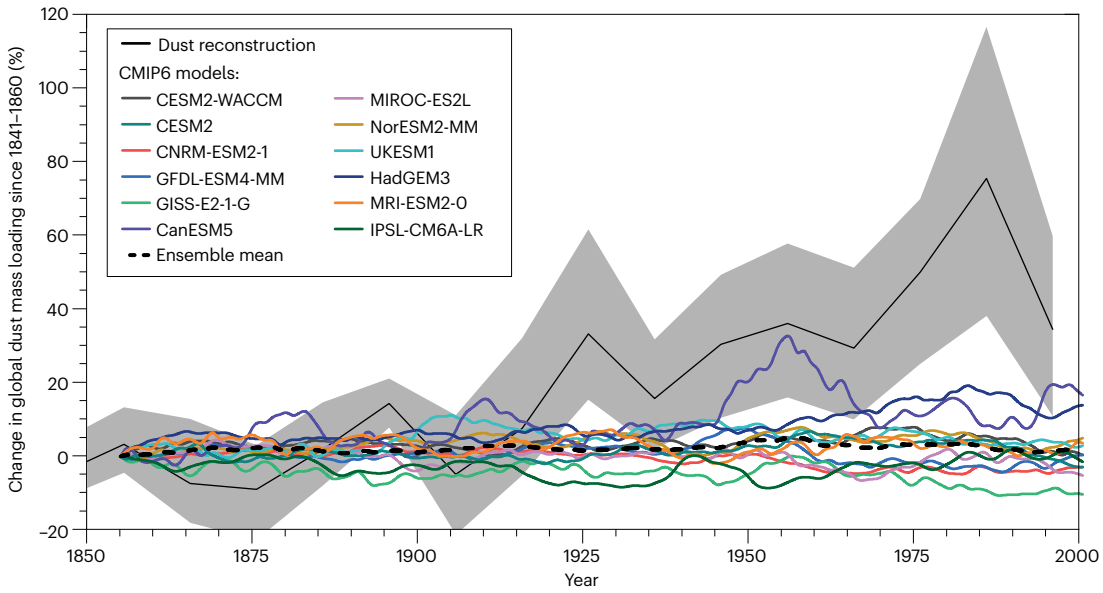

Fig. 5 | Climate model representations of historical changes in dust loading. Changes in global dust loading relative to 1841–1860 from the dust reconstruction (solid black line) and 12 CMIP6 models with prognostic dust aerosol cycles[187] (coloured lines, and dashed black line for the ensemble mean). CMIP6 data are 10-year running means from historical runs[204]. Grey shading denotes the 90% confidence interval for the dust reconstruction. All models and the ensemble mean fail to reproduce the large historical increase in dust loading.

assessments of climate sensitivity and projections of future climate[169,191]. Additional research is thus needed to better constrain R and $\Delta F_{p\rightarrow m}$ and to enable climate models to reproduce the historical increase in dust.

The dust DRE contributes most to the uncertainty in R and $\Delta F_{p\rightarrow m}$ (Fig. 3). Future research should thus focus on reducing its uncertainty by better constraining dust optical properties through in situ and remote-sensing observations. For instance, the information on soil mineralogy to be provided by the Earth Surface Mineral Dust Source Investigation mission of NASA could help constrain dust optical properties[192]. Additionally, models likely underestimate the atmospheric concentration of super-coarse dust greatly[5,6,47,53]. This limitation should be addressed by obtaining more measurements of emitted and transported dust that extend to the difficult-to-measure super-coarse dust size range[6,28,33,52] and by developing improved parameterizations of super-coarse dust emission[193] and deposition and implementing those in climate models.

Another priority for future research is better constraining the radiative effects of dust owing to interactions with clouds, anthropogenic aerosols and biogeochemistry, together contributing the remaining uncertainty in R. Owing to the dearth of observational constraints, the assessment of radiative effects here mostly used modelling studies. However, models struggle to correctly account for interactions of dust with clouds and anthropogenic aerosols, in part because of the mismatch in scales between the relevant processes and climate model grid boxes[35,194,195]. As such, there is an urgent need for comprehensive in situ and satellite observations to constrain these interactions[13,167]. For instance, more satellite and in situ observations of cirrus interactions with dust and other INPs[91,92] could elucidate the relative importance of homogeneous and heterogeneous nucleation of ice crystals, which determines the sign of the radiative effect of dust interactions with cirrus[13] (Fig. 2e). Furthermore, dust radiative effects due to interactions with clouds could be better constrained with future model simulations at a sufficiently high (kilometre-scale[195]) resolution to resolve critical subgrid scale turbulence and cloud processes that are currently parameterized[194]. Finally, constraining radiative effects due to dust interactions with biogeochemistry requires an improved characterization of dust composition and how this evolves during transport, as well as accurate knowledge of which land and ocean regions are nutrient-limited[136].

We also recommend that the community conducts multimodel experiments to obtain robust estimates of the various dust radiative effects and of R and $\Delta F_{p\rightarrow m}$. These experiments should investigate the uncertainty in radiative effects that result from model differences in dust optical properties, size distribution, model resolution, meteorology, the spatiotemporal distribution of dust emission fluxes and parameterizations for dust deposition and dust interactions. Such multimodel experiments could be done in the context of the Aerosol Model Intercomparison project (AeroCom)[26,196].

Future research should also prioritize addressing the failure of models to reproduce the historical increase in dust (Fig. 5). Doing so requires an improved understanding of the factors driving changes in the atmospheric dust loading, including the relative roles of changes in land use, wind speed, soil properties, sediment supply and vegetation cover[155,197]. Additionally, new observations and modelling are needed to clarify the meteorological processes that generate the high wind speeds that produce dust, such as cold pool outflows from moist convection[198–200], and to improve the representation of those processes in climate models. Finally, more physically based dust emission schemes need to be developed and implemented into climate models. These schemes should explicitly account for dust emissions from high latitudes, which have an outsize effect on climate through interactions with clouds[167,168]. Furthermore, dust emission schemes should avoid using empirical dust source functions as these do not respond to changes in climate; instead, emission schemes should use process understanding to account for the dependence of the spatiotemporal pattern and mineralogical composition of dust emissions on wind, soil properties, sediment supply and vegetation coverage[163,201,202]. A challenge will be to achieve this without making these schemes too sensitive to parameters such as soil moisture that nonlinearly increase dust emissions[1,2] and that have considerable variability in climate models[170]. These fundamental improvements in dust emission schemes are also needed for meaningful predictions of future changes in dust and for more accurate predictions of dust impacts on regional climate.

Data availability

The data for the dust reconstruction in Figs 4 and 5 are available at https://doi.org/10.15144/S4VC7X.

Published online: 17 January 2023

References

1. Shao, Y. P. *Physics and Modelling of Wind Erosion* 2nd edn (Springer, 2008).
2. Kok, J. F., Parteli, E. J. R., Michaels, T. I. & Karam, D. B. The physics of wind-blown sand and dust. *Rep. Prog. Phys.* **75**, 106901 (2012).
3. Gillette, D. A. On the production of soil wind erosion having the potential for long range transport. *J. Rech. Atmos.* **8**, 734–744 (1974).
4. Kok, J. F. A scaling theory for the size distribution of emitted dust aerosols suggests climate models underestimate the size of the global dust cycle. *Proc. Natl Acad. Sci. USA* **108**, 1016–1021 (2011).
5. Ryder, C. L. et al. Coarse and giant particles are ubiquitous in Saharan dust export regions and are radiatively significant over the Sahara. *Atmos. Chem. Phys.* **19**, 15353–15376 (2019).
6. Weinzierl, B. et al. The Saharan Aerosol Long-range Transport and Aerosol–Cloud Interaction Experiment (SALTRACE): overview and selected highlights. *Bull. Am. Meteorol. Soc.* **98**, 1427–1451 (2017).
7. Kok, J. F. et al. Smaller desert dust cooling effect estimated from analysis of dust size and abundance. *Nat. Geosci.* **10**, 274–278 (2017).
This article showed that atmospheric dust is coarser than represented in climate models, causing the dust direct radiative effect to be less cooling than thought.
8. Gliss, J. et al. AeroCom phase III multi-model evaluation of the aerosol life cycle and optical properties using ground- and space-based remote sensing as well as surface in situ observations. *Atmos. Chem. Phys.* **21**, 87–128 (2021).
9. Kok, J. F. et al. Contribution of the world's main dust source regions to the global cycle of desert dust. *Atmos. Chem. Phys.* **21**, 8169–8193 (2021).
10. Bullard, J. E. et al. High-latitude dust in the Earth system. *Rev. Geophys.* **54**, 447–485 (2016).
11. Prospero, J. M., Delany, A. C. & Carlson, T. N. The discovery of African dust transport to the Western Hemisphere and the Saharan air layer. *Bull. Am. Meteorol. Soc.* **102**, E1239–E1260 (2021).
12. Highwood, E. J. & Ryder, C. L. in *Mineral Dust: A Key Player in the Earth System* (eds Peter, K. & Jan-Berend, W. S.) 327–357 (Springer Netherlands, 2014).
13. Storelvmo, T. Aerosol effects on climate via mixed-phase and ice clouds. *Annu. Rev. Earth Planet. Sci.* **45**, 199–222 (2017).
14. Karydis, V. A. et al. Global impact of mineral dust on cloud droplet number concentration. *Atmos. Chem. Phys.* **17**, 5601–5621 (2017).
This article investigates the different mechanisms by which dust particles affect warm clouds, finding that dust increases cloud droplet number concentrations over deserts but decreases it over polluted regions.
15. Klingmuller, K., Karydis, V. A., Bacer, S., Stenchikov, G. L. & Lelieveld, J. Weaker cooling by aerosols due to dust–pollution interactions. *Atmos. Chem. Phys.* **20**, 15285–15295 (2020).
16. Klingmuller, K., Lelieveld, J., Karydis, V. A. & Stenchikov, G. L. Direct radiative effect of dust–pollution interactions. *Atmos. Chem. Phys.* **19**, 7397–7408 (2019).
This article uses a chemistry–climate model to shed light on the climatic effects of the interactions between dust and anthropogenic air pollution.
17. Bauer, S. E. et al. Do sulfate and nitrate coatings on mineral dust have important effects on radiative properties and climate modeling? *J. Geophys. Res. Atmos.* https://doi.org/10.1029/2005jd006977 (2007).
This article provides a first attempt to evaluate the effects of dust coating by sulfate and nitrate on the aerosol direct radiative effect.
18. Usher, C. R., Michel, A. E. & Grassian, V. H. Reactions on mineral dust. *Chem. Rev.* **103**, 4883–4939 (2003).
This article provides a comprehensive review of heterogeneous reactions of atmospheric trace gases on mineral dust surface in the troposphere.

19. Skiles, S. M., Flanner, M., Cook, J. M., Dumont, M. & Painter, T. H. Radiative forcing by light-absorbing particles in snow. *Nat. Clim. Change* **8**, 965 (2018).
This article reviews and summarizes the global radiative forcing by dust on snow and ice constrained by observations.
20. Tuccella, P., Pitari, G., Colaiuda, V., Raparelli, E. & Curci, G. Present-day radiative effect from radiation-absorbing aerosols in snow. *Atmos. Chem. Phys.* **21**, 6875–6893 (2021).
This article provides an observationally constrained estimate of the global mean dust-snow radiative effect with a comprehensive uncertainty analysis.
21. Mahowald, N. Aerosol indirect effect on biogeochemical cycles and climate. *Science* **334**, 794–796 (2011).
22. McGraw, Z., Storelvmo, T., David, R. O. & Sagoo, N. Global radiative impacts of mineral dust perturbations through stratiform clouds. *J. Geophys. Res. Atmos.* https://doi.org/10.1029/2019jd031807 (2020).
This global modelling study of the various dust radiative effects on clouds finds that many of the interactions produce counteracting radiative effects.
23. Mahowald, N. M. et al. Observed 20th century desert dust variability: impact on climate and biogeochemistry. *Atmos. Chem. Phys.* **10**, 10875–10893 (2010).
24. Hooper, J. & Marx, S. A global doubling of dust emissions during the Anthropocene. *Glob. Planet. Change* **169**, 70–91 (2018).
This article compiles sedimentary records that recorded dust deposition from pre-industrial times onwards, many of which show approximately a doubling of dust deposition.
25. Boucher, O. & Tanre, D. Estimation of the aerosol perturbation to the Earth's radiative budget over oceans using POLDER satellite aerosol retrievals. *Geophys. Res. Lett.* **27**, 1103–1106 (2000).
26. Boucher, O. et al. in *Climate Change 2013: The Physical Science Basis. Contribution of Working Group I to the Fifth Assessment Report of the Intergovernmental Panel on Climate Change* (eds Stocker, T. F. et al.) 571–658 (Cambridge Univ. Press, 2013).
27. Forster, P. et al. in *Climate Change 2007: The Physical Science Basis* (eds Solomon, S. et al.) (Cambridge Univ. Press, 2007).
28. Ryder, C. L. et al. Optical properties of Saharan dust aerosol and contribution from the coarse mode as measured during the Fennec 2011 aircraft campaign. *Atmos. Chem. Phys.* **13**, 303–325 (2013).
29. Tegen, I. & Lacis, A. A. Modeling of particle size distribution and its influence on the radiative properties of mineral dust aerosol. *J. Geophys. Res. Atmos.* **101**, 19237–19244 (1996).
30. Sokolik, I. N. & Toon, O. B. Incorporation of mineralogical composition into models of the radiative properties of mineral aerosol from UV to IR wavelengths. *J. Geophys. Res. Atmos.* **104**, 9423–9444 (1999).
31. Di Biagio, C., Balkanski, Y., Albani, S., Boucher, O. & Formenti, P. Direct radiative effect by mineral dust aerosols constrained by new microphysical and spectral optical data. *Geophys. Res. Lett.* https://doi.org/10.1029/2019gl086186 (2020).
32. Dufresne, J. L., Gautier, C., Ricchiazzi, P. & Fouquart, Y. Longwave scattering effects of mineral aerosols. *J. Atmos. Sci.* **59**, 1959–1966 (2002).
This article showed that longwave scattering by dust produces a substantial radiative effect that is neglected by climate models.
33. Adebiyi, A. A. et al. A review of coarse mineral dust in the Earth system. Preprint at *EarthArXiv* https://doi.org/10.31223/X5QD36 (2022).
34. Di Biagio, C. et al. Complex refractive indices and single-scattering albedo of global dust aerosols in the shortwave spectrum and relationship to size and iron content. *Atmos. Chem. Phys.* **19**, 15503–15531 (2019).
This article used laboratory experiments to obtain the shortwave optical properties of aerosols generated from desert soil samples across the world, finding that dust in climate models might be too absorbing.
35. Riemer, N., Ault, A. P., West, M., Craig, R. L. & Curtis, J. H. Aerosol mixing state: measurements, modeling, and impacts. *Rev. Geophys.* **57**, 187–249 (2019).
36. Renard, J. B. et al. In situ measurements of desert dust particles above the western Mediterranean Sea with the balloon-borne Light Optical Aerosol Counter/sizer (LOAC) during the ChArMEx campaign of summer 2013. *Atmos. Chem. Phys.* **18**, 3677–3699 (2018).
37. Denjean, C. et al. Size distribution and optical properties of African mineral dust after intercontinental transport. *J. Geophys. Res. Atmos.* **121**, 7117–7138 (2016).
38. Seinfeld, J. H. et al. ACE-ASIA — regional climatic and atmospheric chemical effects of Asian dust and pollution. *Bull. Am. Meteorol. Soc.* **85**, 367–380 (2004).
39. Liao, H. & Seinfeld, J. H. Radiative forcing by mineral dust aerosols: sensitivity to key variables. *J. Geophys. Res. Atmos.* **103**, 31637–31645 (1998).
40. Liou, K. N. *An Introduction to Atmospheric Radiation*. 2nd edn (Academic Press, 2002).
41. Claquin, T., Schulz, M., Balkanski, Y. & Boucher, O. Uncertainties in assessing radiative forcing by mineral dust. *Tellus Ser. B Chem. Phys. Meteorol.* **50**, 491–505 (1998).
42. Kok, J. F. et al. Improved representation of the global dust cycle using observational constraints on dust properties and abundance. *Atmos. Chem. Phys.* **21**, 8127–8167 (2021).
43. Di Biagio, C. et al. Global scale variability of the mineral dust long-wave refractive index: a new dataset of in situ measurements for climate modeling and remote sensing. *Atmos. Chem. Phys.* **17**, 1901–1929 (2017).
44. Li, L. L. et al. Quantifying the range of the dust direct radiative effect due to source mineralogy uncertainty. *Atmos. Chem. Phys.* **21**, 3973–4005 (2021).
45. Sicard, M., Bertolin, S., Mallet, M., Dubuisson, P. & Comeron, A. Estimation of mineral dust long-wave radiative forcing: sensitivity study to particle properties and application to real cases in the region of Barcelona. *Atmos. Chem. Phys.* **14**, 9213–9231 (2014).
46. Brindley, H. E. & Russell, J. E. An assessment of Saharan dust loading and the corresponding cloud-free longwave direct radiative effect from geostationary satellite observations. *J. Geophys. Res. Atmos.* https://doi.org/10.1029/2008jd011635 (2009).
47. Adebiyi, A. A. & Kok, J. F. Climate models miss most of the coarse dust in the atmosphere. *Sci. Adv.* **6**, eaaz9507 (2020).
48. Tuccella, P., Curci, G., Pitari, G., Lee, S. & Jo, D. S. Direct radiative effect of absorbing aerosols: sensitivity to mixing state, brown carbon, and soil dust refractive index and shape. *J. Geophys. Res. Atmos.* https://doi.org/10.1029/2019jd030967 (2020).
49. Albani, S. et al. Improved dust representation in the Community Atmosphere Model. *J. Adv. Model. Earth Syst.* **6**, 541–570 (2014).
50. Ito, A., Adebiyi, A. A., Huang, Y. & Kok, J. F. Less atmospheric radiative heating by dust due to the synergy of coarser size and aspherical shape. *Atmos. Chem. Phys.* **21**, 16869–16891 (2021).
51. Colarco, P. R. et al. Impact of radiatively interactive dust aerosols in the NASA GEOS-5 climate model: sensitivity to dust particle shape and refractive index. *J. Geophys. Res. Atmos.* **119**, 753–786 (2014).
52. Ryder, C. L. et al. Coarse-mode mineral dust size distributions, composition and optical properties from AER-D aircraft measurements over the tropical eastern Atlantic. *Atmos. Chem. Phys.* **18**, 17225–17257 (2018).
53. Ansmann, A. et al. Profiling of Saharan dust from the Caribbean to West Africa, Part 2: shipborne lidar measurements versus forecasts. *Atmos. Chem. Phys. Discuss.* https://doi.org/10.5194/acp-2017-502 (2017).
54. Song, Q. et al. Toward an observation-based estimate of dust net radiative effects in tropical north atlantic through integrating satellite observations and in situ measurements of dust properties. *Atmos. Chem. Phys.* https://doi.org/10.5194/acp-2018-267 (2018).
55. O'Sullivan, D. et al. Models transport Saharan dust too low in the atmosphere: a comparison of the MetUM and CAMS forecasts with observations. *Atmos. Chem. Phys.* **20**, 12955–12982 (2020).
56. Kim, D. et al. Sources, sinks, and transatlantic transport of North African dust aerosol: a multimodel analysis and comparison with remote sensing data. *J. Geophys. Res. Atmos.* **119**, 6259–6277 (2014).
57. Begue, N. et al. Aerosol processing and CCN formation of an intense Saharan dust plume during the EUCAARI 2008 campaign. *Atmos. Chem. Phys.* **15**, 3497–3516 (2015).
58. Formenti, P., Elbert, W., Maenhaut, W., Haywood, J. & Andreae, M. O. Chemical composition of mineral dust aerosol during the Saharan Dust Experiment (SHADE) airborne campaign in the Cape Verde region, September 2000. *J. Geophys. Res. Atmos.* https://doi.org/10.1029/2002jd002648 (2003).
59. Karydis, V. A., Tsimpidi, A. P., Pozzer, A., Astitha, M. & Lelieveld, J. Effects of mineral dust on global atmospheric nitrate concentrations. *Atmos. Chem. Phys.* **16**, 1491–1509 (2016).
60. Sullivan, R. C., Guazzotti, S. A., Sodeman, D. A. & Prather, K. A. Direct observations of the atmospheric processing of Asian mineral dust. *Atmos. Chem. Phys.* **7**, 1213–1236 (2007).
61. Huang, X. et al. Pathways of sulfate enhancement by natural and anthropogenic mineral aerosols in China. *J. Geophys. Res. Atmos.* **119**, 14165–14179 (2014).
62. Sullivan, R. C. et al. Mineral dust is a sink for chlorine in the marine boundary layer. *Atmos. Environ.* **41**, 7166–7179 (2007).
63. Feng, T. et al. Summertime ozone formation in Xi'an and surrounding areas, China. *Atmos. Chem. Phys.* **16**, 4323–4342 (2016).
64. Gharibzadeh, M., Bidokhti, A. A. & Alam, K. The interaction of ozone and aerosol in a semi-arid region in the Middle East: ozone formation and radiative forcing implications. *Atmos. Environ.* https://doi.org/10.1016/j.atmosenv.2020.118015 (2021).
65. Usher, C. R., Al-Hosney, H., Carlos-Cuellar, S. & Grassian, V. H. A laboratory study of the heterogeneous uptake and oxidation of sulfur dioxide on mineral dust particles. *J. Geophys. Res. Atmos.* https://doi.org/10.1029/2002jd002051 (2002).
66. Goodman, A. L., Underwood, G. M. & Grassian, V. H. Heterogeneous reaction of NO_2: characterization of gas-phase and adsorbed products from the reaction, $2NO_2(g)+H_2O(a) \rightarrow HONO(g)+HNO_3(a)$ on hydrated silica particles. *J. Phys. Chem. A* **103**, 7217–7223 (1999).
67. Nenes, A., Pandis, S. N., Weber, R. J. & Russell, A. Aerosol pH and liquid water content determine when particulate matter is sensitive to ammonia and nitrate availability. *Atmos. Chem. Phys.* **20**, 3249–3258 (2020).
68. Karydis, V. A., Tsimpidi, A. P., Pozzer, A. & Lelieveld, J. How alkaline compounds control atmospheric aerosol particle acidity. *Atmos. Chem. Phys.* **21**, 14983–15001 (2021).
69. Trochkine, D. et al. Mineral aerosol particles collected in Dunhuang, China, and their comparison with chemically modified particles collected over Japan. *J. Geophys. Res. Atmos.* https://doi.org/10.1029/2002jd003268 (2003).
70. Fitzgerald, E., Ault, A. P., Zauscher, M. D., Mayol-Bracero, O. L. & Prather, K. A. Comparison of the mixing state of long-range transported Asian and African mineral dust. *Atmos. Environ.* **115**, 19–25 (2015).
71. Klingmuller, K. et al. Revised mineral dust emissions in the atmospheric chemistry-climate model EMAC (MESSy 2.52 DU_Astitha1 KKDU2017 patch). *Geosci. Model. Dev.* **11**, 989–1008 (2018).
72. Perlwitz, J. P., Perez Garcia-Pando, C. & Miller, R. L. Predicting the mineral composition of dust aerosols — part 1: representing key processes. *Atmos. Chem. Phys.* **15**, 11593–11627 (2015).
73. Sullivan, R. C. et al. Effect of chemical mixing state on the hygroscopicity and cloud nucleation properties of calcium mineral dust particles. *Atmos. Chem. Phys.* **9**, 3303–3316 (2009).
74. Cziczo, D. J. et al. Deactivation of ice nuclei due to atmospherically relevant surface coatings. *Environ. Res. Lett.* https://doi.org/10.1088/1748-9326/4/4/044013 (2009).

75. Fan, S. M., Horowitz, L. W., Levy, H. & Moxim, W. J. Impact of air pollution on wet deposition of mineral dust aerosols. *Geophys. Res. Lett.* https://doi.org/10.1029/2003gl018501 (2004).
76. Liao, H., Seinfeld, J. H., Adams, P. J. & Mickley, L. J. Global radiative forcing of coupled tropospheric ozone and aerosols in a unified general circulation model. *J. Geophys. Res. Atmos.* **109**, D16207 (2004).
77. Bauer, S. E. & Koch, D. Impact of heterogeneous sulfate formation at mineral dust surfaces on aerosol loads and radiative forcing in the Goddard Institute for Space Studies general circulation model. *J. Geophys. Res. Atmos.* https://doi.org/10.1029/2005jd005870 (2005).
78. Koehler, K. A. et al. Hygroscopicity and cloud droplet activation of mineral dust aerosol. *Geophys. Res. Lett.* https://doi.org/10.1029/2009gl037348 (2009).
79. Kumar, P., Sokolik, I. N. & Nenes, A. Measurements of cloud condensation nuclei activity and droplet activation kinetics of fresh unprocessed regional dust samples and minerals. *Atmos. Chem. Phys.* **11**, 3527–3541 (2011).
80. Gaston, C. J. Re-examining dust chemical aging and its impacts on earth's climate. *Acc. Chem. Res.* **53**, 1005–1013 (2020).
81. Karydis, V. A., Kumar, P., Barahona, D., Sokolik, I. N. & Nenes, A. On the effect of dust particles on global cloud condensation nuclei and cloud droplet number. *J. Geophys. Res. Atmos.* https://doi.org/10.1029/2011jd016283 (2011).
82. Sagoo, N. & Storelvmo, T. Testing the sensitivity of past climates to the indirect effects of dust. *Geophys. Res. Lett.* **44**, 5807–5817 (2017).
83. Li, R., Min, Q. L. & Harrison, L. C. A case study: the indirect aerosol effects of mineral dust on warm clouds. *J. Atmos. Sci.* **67**, 805–816 (2010).
84. Hoose, C. & Mohler, O. Heterogeneous ice nucleation on atmospheric aerosols: a review of results from laboratory experiments. *Atmos. Chem. Phys.* **12**, 9817–9854 (2012).
85. Kanji, Z. A. et al. Overview of ice nucleating particles. *Meteorol. Monogr.* https://doi.org/10.1175/amsmonographs-d-16-0006.1 (2017).
86. Matus, A. V. & L'Ecuyer, T. S. The role of cloud phase in Earth's radiation budget. *J. Geophys. Res. Atmos.* **122**, 2559–2578 (2017).
87. Morrison, H. et al. Resilience of persistent Arctic mixed-phase clouds. *Nat. Geosci.* **5**, 11–17 (2012).
88. Shi, Y. & Liu, X. H. Dust radiative effects on climate by glaciating mixed-phase clouds. *Geophys. Res. Lett.* **46**, 6128–6137 (2019).
This global modelling study finds that dust-induced glaciation of mixed-phase clouds produces net warming globally but cooling in the Arctic.
89. Choi, Y. S., Lindzen, R. S., Ho, C. H. & Kim, J. Space observations of cold-cloud phase change. *Proc. Natl Acad. Sci. USA* **107**, 11211–11216 (2010).
90. Tan, I., Storelvmo, T. & Choi, Y. S. Spaceborne lidar observations of the ice-nucleating potential of dust, polluted dust, and smoke aerosols in mixed-phase clouds. *J. Geophys. Res. Atmos.* **119**, 6653–6665 (2014).
91. Froyd, K. D. et al. Dominant role of mineral dust in cirrus cloud formation revealed by global-scale measurements. *Nat. Geosci.* **15**, 177 (2022).
This article combined observations and modelling to demonstrate the importance of dust for nucleating cirrus clouds.
92. Cziczo, D. J. et al. Clarifying the dominant sources and mechanisms of cirrus cloud formation. *Science* **340**, 1320–1324 (2013).
93. David, R. O. et al. Pore condensation and freezing is responsible for ice formation below water saturation for porous particles. *Proc. Natl Acad. Sci. USA* **116**, 8184–8189 (2019).
94. Heymsfield, A. J. et al. Cirrus clouds. *Meteorol. Monogr.* https://doi.org/10.1175/amsmonographs-d-16-0010.1 (2017).
95. Storelvmo, T. & Herger, N. Cirrus cloud susceptibility to the injection of ice nuclei in the upper troposphere. *J. Geophys. Res. Atmos.* **119**, 2375–2389 (2014).
96. Ullrich, R. et al. A new ice nucleation active site parameterization for desert dust and soot. *J. Atmos. Sci.* **74**, 699–717 (2017).
97. Liu, X. et al. Sensitivity studies of dust ice nuclei effect on cirrus clouds with the Community Atmosphere Model CAM5. *Atmos. Chem. Phys.* **12**, 12061–12079 (2012).
98. Huang, J. P., Wang, T. H., Wang, W. C., Li, Z. Q. & Yan, H. R. Climate effects of dust aerosols over East Asian arid and semiarid regions. *J. Geophys. Res. Atmos.* **119**, 11398–11416 (2014).
99. Perlwitz, J. & Miller, R. L. Cloud cover increase with increasing aerosol absorptivity: a counterexample to the conventional semidirect aerosol effect. *J. Geophys. Res. Atmos.* https://doi.org/10.1029/2009jd012637 (2010).
100. Amiri-Farahani, A., Allen, R. J., Neubauer, D. & Lohmann, U. Impact of Saharan dust on North Atlantic marine stratocumulus clouds: importance of the semidirect effect. *Atmos. Chem. Phys.* **17**, 6305–6322 (2017).
101. Ackerman, A. S. et al. Reduction of tropical cloudiness by soot. *Science* **288**, 1042–1047 (2000).
This article shows that absorbing aerosols within a cloud layer can reduce cloudiness.
102. Sand, M. et al. Aerosol absorption in global models from AeroCom phase III. *Atmos. Chem. Phys.* **21**, 15929–15947 (2021).
103. Samset, B. H. et al. Aerosol absorption: progress towards global and regional constraints. *Curr. Clim. Change Rep.* **4**, 65–83 (2018).
104. Doherty, O. M. & Evan, A. T. Identification of a new dust-stratocumulus indirect effect over the tropical North Atlantic. *Geophys. Res. Lett.* **41**, 6935–6942 (2014).
105. Huang, J. P. et al. Satellite-based assessment of possible dust aerosols semi-direct effect on cloud water path over East Asia. *Geophys. Res. Lett.* https://doi.org/10.1029/2006gl026561 (2006).
106. McFarquhar, G. M. & Wang, H. L. Effects of aerosols on trade wind cumuli over the Indian Ocean: model simulations. *Q. J. R. Meteorol. Soc.* **132**, 821–843 (2006).
107. Feingold, G., Jiang, H. L. & Harrington, J. Y. On smoke suppression of clouds in Amazonia. *Geophys. Res. Lett.* https://doi.org/10.1029/2004gl021369 (2005).
108. Stephens, G. L., Wood, N. B. & Pakula, L. A. On the radiative effects of dust on tropical convection. *Geophys. Res. Lett.* https://doi.org/10.1029/2004gl021342 (2004).
109. Wong, S., Dessler, A. E., Mahowald, N. M., Yang, P. & Feng, Q. Maintenance of lower tropospheric temperature inversion in the saharan air layer by dust and dry anomaly. *J. Clim.* **22**, 5149–5162 (2009).
110. Zhu, A., Ramanathan, V., Li, F. & Kim, D. Dust plumes over the Pacific, Indian, and Atlantic oceans: climatology and radiative impact. *J. Geophys. Res. Atmos.* https://doi.org/10.1029/2007jd008427 (2007).
111. Chen, S. H., Wang, S. H. & Waylonis, M. Modification of Saharan air layer and environmental shear over the eastern Atlantic Ocean by dust-radiation effects. *J. Geophys. Res. Atmos.* **115**, D21202 (2010).
112. Huang, J. P. et al. Possible influences of Asian dust aerosols on cloud properties and radiative forcing observed from MODIS and CERES. *Geophys. Res. Lett.* https://doi.org/10.1029/2005gl024724 (2006).
113. Amiri-Farahani, A., Allen, R. J., Li, K. F. & Chu, J. E. The semidirect effect of combined dust and sea salt aerosols in a multimodel analysis. *Geophys. Res. Lett.* **46**, 10512–10521 (2019).
114. Tegen, I. & Heinold, B. Large-scale modeling of absorbing aerosols and their semi-direct effects. *Atmosphere* https://doi.org/10.3390/atmos9100380 (2018).
115. Painter, T. H. et al. Response of Colorado River runoff to dust radiative forcing in snow. *Proc. Natl Acad. Sci. USA* **107**, 17125–17130 (2010).
116. Hall, A. The role of surface albedo feedback in climate. *J. Clim.* **17**, 1550–1568 (2004).
117. Flanner, M. G. et al. Springtime warming and reduced snow cover from carbonaceous particles. *Atmos. Chem. Phys.* **9**, 2481–2497 (2009).
118. Dang, C., Brandt, R. E. & Warren, S. G. Parameterizations for narrowband and broadband albedo of pure snow and snow containing mineral dust and black carbon. *J. Geophys. Res. Atmos.* **120**, 5446–5468 (2015).
119. Flanner, M. G. et al. SNICAR-ADv3: a community tool for modeling spectral snow albedo. *Geosci. Model. Dev.* **14**, 7673–7704 (2021).
120. Liou, K. N. et al. Stochastic parameterization for light absorption by internally mixed BC/dust in snow grains for application to climate models. *J. Geophys. Res. Atmos.* **119**, 7616–7632 (2014).
121. He, C. L., Liou, K. N., Takano, Y., Chen, F. & Barlage, M. Enhanced snow absorption and albedo reduction by dust-snow internal mixing: modeling and parameterization. *J. Adv. Model. Earth Syst.* **11**, 3755–3776 (2019).
122. Warren, S. G. & Wiscombe, W. J. A model for the spectral albedo of snow .2. Snow containing atmospheric aerosols. *J. Atmos. Sci.* **37**, 2734–2745 (1980).
123. He, C., Takano, Y. & Liou, K. N. Close packing effects on clean and dirty snow albedo and associated climatic implications. *Geophys. Res. Lett.* **44**, 3719–3727 (2017).
124. He, C. & Flanner, M. *Snow albedo and radiative transfer: theory, modeling, and parameterization* 67–133 (Springer, 2020). [Series Ed Kokhanovsky, A. Springer Series in Light Scattering]
125. Dang, C. et al. Measurements of light-absorbing particles in snow across the Arctic, North America, and China: effects on surface albedo. *J. Geophys. Res. Atmos.* **122**, 10149–10168 (2017).
126. Kylling, A., Zwaaftink, C. D. G. & Stohl, A. Mineral dust instantaneous radiative forcing in the Arctic. *Geophys. Res. Lett.* **45**, 4290–4298 (2018).
127. Dong, Z. W. et al. Aeolian dust transport, cycle and influences in high-elevation cryosphere of the Tibetan Plateau region: new evidences from alpine snow and ice. *Earth Sci. Rev.* https://doi.org/10.1016/j.earscirev.2020.103408 (2020).
128. Di Mauro, B. et al. Mineral dust impact on snow radiative properties in the European Alps combining ground, UAV, and satellite observations. *J. Geophys. Res. Atmos.* **120**, 6080–6097 (2015).
129. Skiles, S. M. & Painter, T. H. Toward understanding direct absorption and grain size feedbacks by dust radiative forcing in snow with coupled snow physical and radiative transfer modeling. *Water Resour. Res.* **55**, 7362–7378 (2019).
130. Lawrence, D. M. et al. The CCSM4 Land Simulation, 1850–2005: assessment of surface climate and new capabilities. *J. Clim.* **25**, 2240–2260 (2012).
131. Martin, J. H. Glacial-interglacial CO_2 change: the iron hypothesis. *Paleoceanography* **5**, 1–13 (1990).
132. Moore, C. M. et al. Processes and patterns of oceanic nutrient limitation. *Nat. Geosci.* **6**, 701–710 (2013).
This article reviews the current understanding of limiting nutrients for ocean ecosystems.
133. Capone, D. G., Zehr, J. P., Paerl, H. W., Bergman, B. & Carpenter, E. J. *Trichodesmium*, a globally significant marine cyanobacterium. *Science* **276**, 1221–1229 (1997).
134. Moore, J. K., Doney, S. C., Lindsay, K., Mahowald, N. & Michaels, A. F. Nitrogen fixation amplifies the ocean biogeochemical response to decadal timescale variations in mineral dust deposition. *Tellus Ser. B Chem. Phys. Meteorol.* **58**, 560–572 (2006).
135. Johnson, M. S. & Meskhidze, N. Atmospheric dissolved iron deposition to the global oceans: effects of oxalate-promoted Fe dissolution, photochemical redox cycling, and dust mineralogy. *Geosci. Model. Dev.* **6**, 1137–1155 (2013).
136. Mahowald, N. M. et al. Aerosol trace metal leaching and impacts on marine microorganisms. *Nat. Commun.* https://doi.org/10.1038/s41467-018-04970-7 (2018).
137. Tagliabue, A. et al. The integral role of iron in ocean biogeochemistry. *Nature* **543**, 51–59 (2017).
138. Krishnamurthy, A., Moore, J. K., Mahowald, N., Luo, C. & Zender, C. S. Impacts of atmospheric nutrient inputs on marine biogeochemistry. *J. Geophys. Res. Biogeosci.* https://doi.org/10.1029/2009jg001115 (2010).

139. Mahowald, N. et al. Desert dust and anthropogenic aerosol interactions in the Community Climate System Model coupled-carbon-climate model. *Biogeosciences* **8**, 387–414 (2011).
140. Okin, G. S. et al. Spatial patterns of soil nutrients in two southern African savannas. *J. Geophys. Res. Biogeosci.* https://doi.org/10.1029/2007jg000584 (2008).
141. Vitousek, P. M. Litterfall, nutrient cycling, and nutrient limitation in tropical forests. *Ecology* **65**, 285–298 (1984).
142. Falkowski, P. G., Barber, R. T. & Smetacek, V. Biogeochemical controls and feedbacks on ocean primary production. *Science* **281**, 200–206 (1998).
143. Swap, R., Garstang, M., Greco, S., Talbot, R. & Kallberg, P. Saharan dust in the Amazon basin. *Tellus Ser. B Chem. Phys. Meteorol.* **44**, 133–149 (1992).
144. Okin, G. S., Mahowald, N., Chadwick, O. A. & Artaxo, P. Impact of desert dust on the biogeochemistry of phosphorus in terrestrial ecosystems. *Glob. Biogeochem. Cycles* **18**, Gb2005 (2004).
145. Armstrong, R. A., Lee, C., Hedges, J. I., Honjo, S. & Wakeham, S. G. A new, mechanistic model for organic carbon fluxes in the ocean based on the quantitative association of POC with ballast minerals. *Deep Sea Res. Part II-Top. Stud. Oceanogr.* **49**, 219–236 (2001).
146. van der Jagt, H., Friese, C., Stuut, J. B. W., Fischer, G. & Iversen, M. H. The ballasting effect of Saharan dust deposition on aggregate dynamics and carbon export: aggregation, settling, and scavenging potential of marine snow. *Limnol. Oceanogr.* **63**, 1386–1394 (2018).
147. Paytan, A. et al. Toxicity of atmospheric aerosols on marine phytoplankton. *Proc. Natl Acad. Sci. USA* **106**, 4601–4605 (2009).
148. Thornhill, G. D. et al. Effective radiative forcing from emissions of reactive gases and aerosols — a multi-model comparison. *Atmos. Chem. Phys.* **21**, 853–874 (2021).
149. Patadia, F., Yang, E. S. & Christopher, S. A. Does dust change the clear sky top of atmosphere shortwave flux over high surface reflectance regions? *Geophys. Res. Lett.* **36**, L15825 (2009).
150. McConnell, J. R., Aristarain, A. J., Banta, J. R., Edwards, P. R. & Simoes, J. C. 20th-Century doubling in dust archived in an Antarctic Peninsula ice core parallels climate change and desertification in South America. *Proc. Natl Acad. Sci. USA* **104**, 5743–5748 (2007).
151. Mulitza, S. et al. Increase in African dust flux at the onset of commercial agriculture in the Sahel region. *Nature* **466**, 226–228 (2010).
152. Clifford, H. M. et al. A 2000 year saharan dust event proxy record from an ice core in the European Alps. *J. Geophys. Res. Atmos.* **124**, 12882–12900 (2019).
153. Prospero, J. M. & Lamb, P. J. African droughts and dust transport to the Caribbean: climate change implications. *Science* **302**, 1024–1027 (2003).
154. Evan, A. T. & Mukhopadhyay, S. African dust over the Northern Tropical Atlantic: 1955–2008. *J. Appl. Meteorol. Climatol.* **49**, 2213–2229 (2010).
155. Evan, A. T., Flamant, C., Gaetani, M. & Guichard, F. The past, present and future of African dust. *Nature* **531**, 493–495 (2016).
156. Mahowald, N. M., Ballantine, J. A., Feddema, J. & Ramankutty, N. Global trends in visibility: implications for dust sources. *Atmos. Chem. Phys.* **7**, 3309–3339 (2007).
157. Shao, Y. P., Klose, M. & Wyrwoll, K. H. Recent global dust trend and connections to climate forcing. *J. Geophys. Res. Atmos.* **118**, 11107–11118 (2013).
158. Wang, X., Huang, J. P., Ji, M. X. & Higuchi, K. Variability of East Asia dust events and their long-term trend. *Atmos. Environ.* **42**, 3156–3165 (2008).
159. Zuidema, P. et al. Is summer African dust arriving earlier to Barbados? The updated long-term in situ dust mass concentration time series from ragged point, Barbados, and Miami, Florida. *Bull. Am. Meteorol. Soc.* **100**, 1981–1986 (2019).
160. Gkikas, A. et al. Quantification of the dust optical depth across spatiotemporal scales with the MIDAS global dataset (2003–2017). *Atmos. Chem. Phys.* **22**, 3553–3578 (2022).
161. Ginoux, P. et al. Sources and distributions of dust aerosols simulated with the GOCART model. *J. Geophys. Res.* **106**, 20255–20273 (2001).
162. Wu, C. C., Lin, Z. & Liu, X. The global dust cycle and uncertainty in CMIP5 (Coupled Model Intercomparison Project phase 5) models. *Atmos. Chem. Phys.* **20**, 10401–10425 (2020).
163. Kok, J. F., Albani, S., Mahowald, N. M. & Ward, D. S. An improved dust emission model — part 2: evaluation in the Community Earth System Model, with implications for the use of dust source functions. *Atmos. Chem. Phys.* **14**, 13043–13061 (2014).
164. Forster, P. et al. in *The Earth's Energy Budget, Climate Feedbacks, and Climate Sensitivity* (eds Masson-Delmotte, V. et al.) Ch. 7 (Cambridge Univ. Press, 2021).
This chapter provides a comprehensive review of how Earth's energy budget has been perturbed by anthropogenic emissions of greenhouse gases and aerosols.
165. Stevens, B. Rethinking the lower bound on aerosol radiative forcing. *J. Clim.* **28**, 4794–4819 (2015).
166. Carslaw, K. S. et al. Large contribution of natural aerosols to uncertainty in indirect forcing. *Nature* **503**, 67–71 (2013).
167. Murray, B. J., Carslaw, K. S. & Field, P. R. Opinion: cloud-phase climate feedback and the importance of ice-nucleating particles. *Atmos. Chem. Phys.* **21**, 665–679 (2021).
This article highlights the importance of understanding present and future emissions of dust and other ice nucleating particles for determining the cloud-phase climate feedback that partially controls climate sensitivity.
168. Shi, Y. et al. Relative importance of high-latitude local and long-range-transported dust for Arctic ice-nucleating particles and impacts on Arctic mixed-phase clouds. *Atmos. Chem. Phys.* **22**, 2909–2935 (2022).
169. Sherwood, S. C. et al. An assessment of earth's climate sensitivity using multiple lines of evidence. *Rev. Geophys.* https://doi.org/10.1029/2019rg000678 (2020).
170. Caretta, M. A. et al. in *Climate Change 2022: Impacts, Adaptation, and Vulnerability. Contribution of Working Group II to the Sixth Assessment Report of the Intergovernmental Panel on Climate Change* (eds Pörtner, H.-O. et al.) (Cambridge Univ. Press, 2022).
171. Cook, B. I. et al. Twenty-first century drought projections in the CMIP6 forcing scenarios. *Earth Future* https://doi.org/10.1029/2019ef001461 (2020).
172. Mahowald, N. M. & Luo, C. A less dusty future? *Geophys. Res. Lett.* **30**, 1903 (2003).
173. Smith, W. K. et al. Large divergence of satellite and Earth system model estimates of global terrestrial CO_2 fertilization. *Nat. Clim. Change* **6**, 306–310 (2016).
174. McVicar, T. R. et al. Global review and synthesis of trends in observed terrestrial near-surface wind speeds: implications for evaporation. *J. Hydrol.* **416**, 182–205 (2012).
175. Zha, J. L. et al. Projected changes in global terrestrial near-surface wind speed in 1.5–4.0 °C global warming levels. *Environ. Res. Lett.* https://doi.org/10.1088/1748-9326/ac2fdd (2021).
176. Pendergrass, A. G., Knutti, R., Lehner, F., Deser, C. & Sanderson, B. M. Precipitation variability increases in a warmer climate. *Sci. Rep.* https://doi.org/10.1038/s41598-017-17966-y (2017).
177. O'Gorman, P. A. & Schneider, T. The physical basis for increases in precipitation extremes in simulations of 21st-century climate change. *Proc. Natl Acad. Sci. USA* **106**, 14773–14777 (2009).
178. Zender, C. S. & Kwon, E. Y. Regional contrasts in dust emission responses to climate. *J. Geophys. Res. Atmos.* https://doi.org/10.1029/2004jd005501 (2005).
179. Rodriguez-Caballero, E. et al. Global cycling and climate effects of aeolian dust controlled by biological soil crusts. *Nat. Geosci.* **15**, 458 (2022).
180. Tegen, I., Werner, M., Harrison, S. P. & Kohfeld, K. E. Relative importance of climate and land use in determining present and future global soil dust emission. *Geophys. Res. Lett.* https://doi.org/10.1029/2003gl019216 (2004).
181. Woodward, S., Roberts, D. L. & Betts, R. A. A simulation of the effect of climate change-induced desertification on mineral dust aerosol. *Geophys. Res. Lett.* **32**, L18810 (2005).
182. Mahowald, N. M. et al. Change in atmospheric mineral aerosols in response to climate: last glacial period, preindustrial, modern, and doubled carbon dioxide climates. *J. Geophys. Res.* **111**, D10202 (2006).
183. Evan, A. T., Flamant, C., Fiedler, S. & Doherty, O. An analysis of aeolian dust in climate models. *Geophys. Res. Lett.* **41**, 5996–6001 (2014).
184. Evan, A. T. Surface winds and dust biases in climate models. *Geophys. Res. Lett.* **45**, 1079–1085 (2018).
185. Wu, C. L. et al. Can climate models reproduce the decadal change of dust aerosol in East Asia. *Geophys. Res. Lett.* **45**, 9953–9962 (2018).
186. Pu, B. & Ginoux, P. How reliable are CMIP5 models in simulating dust optical depth. *Atmos. Chem. Phys.* **18**, 12491–12510 (2018).
187. Zhao, A., Ryder, C. L. & Wilcox, L. J. How well do the CMIP6 models simulate dust aerosols? *Atmos. Chem. Phys.* **22**, 2095–2119 (2022).
This article shows that many of the biases reported for simulated dust in CMIP5 climate models still exist in the more recent CMIP6 models and implies that, as model complexity grows, so does the intermodel spread in simulated dust.
188. Thornhill, G. et al. Climate-driven chemistry and aerosol feedbacks in CMIP6 Earth system models. *Atmos. Chem. Phys.* **21**, 1105–1126 (2021).
189. Kok, J. F., Ward, D. S., Mahowald, N. M. & Evan, A. T. Global and regional importance of the direct dust–climate feedback. *Nat. Commun.* https://doi.org/10.1038/s41467-017-02620-y (2018).
This article estimates the dust-climate feedback on global and regional scales using models and observations.
190. Kok, J. F. et al. An improved dust emission model — part 1: model description and comparison against measurements. *Atmos. Chem. Phys.* **14**, 13023–13041 (2014).
191. Andreae, M. O., Jones, C. D. & Cox, P. M. Strong present-day aerosol cooling implies a hot future. *Nature* **435**, 1187–1190 (2005).
This article shows that a strong negative radiative forcing (cooling) due to aerosol changes since pre-industrial times implies a high climate sensitivity.
192. Green, R. O. et al. The Earth surface mineral dust source investigation: an Earth science imaging spectroscopy mission. *IEEE Aerospace Conference* (2020).
193. Meng, J. et al. Improved parameterization for the size distribution of emitted dust aerosols reduces model underestimation of super coarse dust. *Geophys. Res. Lett.* https://doi.org/10.1029/2021gl097287 (2022).
194. The National Academies of Sciences, Engineering, and Medicine. *Reflecting Sunlight: Recommendations for Solar Geoengineering Research and Research Governance* (The National Academies Press, 2021).
195. Slingo, J. et al. Ambitious partnership needed for reliable climate prediction. *Nat. Clim. Change* **12**, 499–503 (2022).
196. Myhre, G. et al. Radiative forcing of the direct aerosol effect from AeroCom Phase II simulations. *Atmos. Chem. Phys.* **13**, 1853–1877 (2013).
197. Okin, G. S. Where and how often does rain prevent dust emission? *Geophys. Res. Lett.* https://doi.org/10.1029/2021gl095501 (2022).
198. Bergametti, G. et al. Rain, wind, and dust connections in the Sahel. *J. Geophys. Res. Atmos.* https://doi.org/10.1029/2021jd035802 (2022).
199. Marsham, J. H., Knippertz, P., Dixon, N. S., Parker, D. J. & Lister, G. M. S. The importance of the representation of deep convection for modeled dust-generating winds over West Africa during summer. *Geophys. Res. Lett.* https://doi.org/10.1029/2011gl048368 (2011).
200. Heinold, B. et al. The role of deep convection and nocturnal low-level jets for dust emission in summertime West Africa: estimates from convection-permitting simulations. *J. Geophys. Res. Atmos.* **118**, 4385–4400 (2013).
201. Okin, G. S. A new model of wind erosion in the presence of vegetation. *J. Geophys. Res. Earth Surf.* **113**, F02s10 (2008).

202. Chappell, A. & Webb, N. P. Using albedo to reform wind erosion modelling, mapping and monitoring. *Aeolian Res.* **23**, 63–78 (2016).
203. Huang, J. P. et al. Global semi-arid climate change over last 60 years. *Clim. Dyn.* **46**, 1131–1150 (2016).
204. Eyring, V. et al. Overview of the Coupled Model Intercomparison Project phase 6 (CMIP6) experimental design and organization. *Geosci. Model. Dev.* **9**, 1937–1958 (2016).
205. Stanelle, T., Bey, I., Raddatz, T., Reick, C. & Tegen, I. Anthropogenically induced changes in twentieth century mineral dust burden and the associated impact on radiative forcing. *J. Geophys. Res. Atmos.* **119**, 13526–13546 (2014).
206. Kohfeld, K. E. & Harrison, S. P. DIRTMAP: the geological record of dust. *Earth Sci. Rev.* **54**, 81–114 (2001).
207. Markle, B. R., Steig, E. J., Roe, G. H., Winckler, G. & McConnell, J. R. Concomitant variability in high-latitude aerosols, water isotopes and the hydrologic cycle. *Nat. Geosci.* **11**, 853 (2018).
208. Cowie, S. M., Knippertz, P. & Marsham, J. H. Are vegetation-related roughness changes the cause of the recent decrease in dust emission from the Sahel? *Geophys. Res. Lett.* **40**, 1868–1872 (2013).
209. Smith, S. D. et al. Elevated CO_2 increases productivity and invasive species success in an arid ecosystem. *Nature* **408**, 79–82 (2000).
210. Goldewijk, K. K., Beusen, A., van Drecht, G. & de Vos, M. The HYDE 3.1 spatially explicit database of human-induced global land-use change over the past 12,000 years. *Glob. Ecol. Biogeogr.* **20**, 73–86 (2011).
211. Lee, J. A., Baddock, M. C., Mbuh, M. J. & Gill, T. E. Geomorphic and land cover characteristics of aeolian dust sources in West Texas and eastern New Mexico, USA. *Aeolian Res.* **3**, 459–466 (2012).
212. Neff, J. C. et al. Increasing eolian dust deposition in the western United States linked to human activity. *Nat. Geosci.* **1**, 189–195 (2008).
213. Webb, N. P. & Pierre, C. Quantifying anthropogenic dust emissions. *Earth Future* **6**, 286–295 (2018).
214. Niemeyer, T. C. et al. Optical depth, size distribution and flux of dust from Owens Lake, California. *Earth Surf. Process. Landf.* **24**, 463–479 (1999).
215. Xi, X. & Sokolik, I. N. Quantifying the anthropogenic dust emission from agricultural land use and desiccation of the Aral Sea in Central Asia. *J. Geophys. Res. Atmos.* **121**, 12270–12281 (2016).
216. Indoitu, R. et al. Dust emission and environmental changes in the dried bottom of the Aral Sea. *Aeolian Res.* **17**, 101–115 (2015).
217. Tegen, I. & Fung, I. Contribution to the atmospheric mineral aerosol load from land-surface modification. *J. Geophys. Res. Atmos.* **100**, 18707–18726 (1995).
218. Sokolik, I. N. & Toon, O. B. Direct radiative forcing by anthropogenic airborne mineral aerosols. *Nature* **381**, 681–683 (1996).
219. Mahowald, N. M., Rivera, G. D. R. & Luo, C. Comment on 'Relative importance of climate and land use in determining present and future global soil dust emission' by I. Tegen et al. *Geophys. Res. Lett.* https://doi.org/10.1029/2004gl021272 (2004).
220. Mahowald, N. M. Anthropocene changes in desert area: sensitivity to climate model predictions. *Geophys. Res. Lett.* **34**, L18817 (2007).
221. Ginoux, P., Prospero, J. M., Gill, T. E., Hsu, N. C. & Zhao, M. Global-scale attribution of anthropogenic and natural dust sources and their emission rates based on MODIS Deep Blue aerosol products. *Rev. Geophys.* **50**, Rg3005 (2012).
This article uses satellite data to attribute dust emissions to natural and anthropogenic sources, finding that anthropogenic emissions account for approximately a quarter of dust emissions.

Acknowledgements
J.F.K. is funded by the National Science Foundation grants 1856389 and 2151093, A.T.E. is funded by NSF grant 1833173, N.M.M. is funded by the Department of Energy grant DE-SC0021302 and V.A.K. and T.S. are supported by the European Union via its Horizon 2020 project FORCeS (GA 81205). We thank J. Hooper and P. Sabatier for providing dust deposition data.

Author contributions
J.F.K. led the review, performed the dust reconstruction, wrote the Supplementary material, prepared the figures and compiled the paper. T.S. and A.A.A. contributed the section on clouds and Fig. 2c–f. V.A.K. contributed the section on atmospheric chemistry and Fig. 2b. N.M.M. contributed the section on biogeochemistry and a draft of Fig. 2h. C.H. contributed the section on the cryosphere and Fig. 2g. A.T.E. contributed the section on future dust changes. D.M.L. contributed to the CMIP6 results in Fig. 5. All authors contributed to the manuscript preparation, discussion and writing.

Competing interests
The authors declare no competing interests.

Additional information
Supplementary information The online version contains supplementary material available at https://doi.org/10.1038/s43017-022-00379-5.

Correspondence should be addressed to Jasper F. Kok.

Peer review information *Nature Reviews Earth & Environment* thanks Bernadett Weinzierl, Peter Colarco and Yves Balkanski for their contribution to the peer review of this work.